https://doi.org/10.5194/esd-2021-9
Preprint. Discussion started: 31 March 2021

Earth System Dynamics Discussions
Open Access
EGU

Downscaling of climate change scenarios for a high resolution, site–specific assessment of drought stress risk for two viticultural regions with heterogeneous landscapes

Marco Hofmann[1], Claudia Volosciuk[2], Martin Dubrovský[3,4], Douglas Maraun[5] and Hans R. Schultz[1]

[1]Department of General and Organic Viticulture, Hochschule Geisenheim University, Geisenheim, 65366, Germany
[2]Science and Innovation Department, World Meteorological Organization, Geneva, CH-1211, Switzerland
[3]Institute of Atmospheric Physics, The Czech Academy of Sciences, Prague, 141 00, Czech Republic
[4]Global Change Research Institute, The Czech Academy of Sciences, Brno, 603 00, Czech Republic
[5]Wegener Center for Climate and Global Change, University of Graz, Graz, 8010, Austria

Correspondence to: Marco Hofmann (marco.hofmann@hs-gm.de)

Abstract. Extended periods without precipitation observed for example in Central Europe including Germany during the seasons from 2018 to 2020, can lead to water deficit and yield and quality losses for grape and wine production. However, irrigation infrastructure is largely non–existent. Regional climate models project changes of precipitation amounts and patterns, indicating an increase in frequency of occurrence of comparable situations in the future. In order to assess possible impacts of climate change on the water budget of grapevines, a water balance model was developed, which accounts for the large heterogeneity of vineyards with respect to their soil water storage capacity, evapotranspiration as a function of slope and aspect, and viticultural management practices. The model was fed with data from soil maps (soil type and plant available water capacity), a digital elevation model, the European Union (EU) vineyard–register, observed weather data and future weather data provided by regional climate models and a stochastic weather generator. This allowed conducting a risk assessment of the drought stress occurrence for the wine–producing regions Rheingau and Hessische Bergstraße in Germany on the scale of individual vineyard plots. The simulations showed that the risk for drought stress varies substantially between vineyard sites but might increase for steep–slope regions in the future. Possible adaptation measures depend highly on local conditions and to make targeted use of the resource water, an intense interplay of different wine-industry stakeholders, research, knowledge transfer, and local authorities will be required.

1 Introduction

Global mean temperature has increased with the strongest observed changes per decade since the 1980s (WMO, 2020). Warming during the growing season (Apr–Oct, Northern Hemisphere, Oct–Apr, Southern Hemisphere) has also been observed in all studied wine regions on several continents over the past 50–60 years (Schultz, 2000; Jones et al., 2005a; Webb et al., 2007, 2011; Santos et al., 2012). Changes in temperature have a pronounced effect on the geographical distribution of where grapevines can be grown (Kenny and Harrison, 1992; Jones et al., 2005b; Schultz and Jones, 2010; Santos et al., 2012), since this crop is highly responsive to environmental conditions (Sadras et al., 2012a). Within the existing production areas, water shortage is probably the most dominant environmental constraint (Williams and Matthews, 1990) and even in moderate temperate climates, grapevines often face some degree of drought stress during the growing season (Morlat et al., 1992; Van Leeuwen and Seguin, 1994; Gaudillère et al., 2002; Gruber and Schultz, 2005; Gruber, 2012). Soil moisture decreased across Europe since the beginning of the 20th century (Hanel et al., 2018) and in the most recent decade, the severity of drought events increased in southwestern Germany (Erfurt et al., 2020). This was in part a consequence of observed recent increases in potential evapotranspiration (Bormann, 2011; Hartmann et al., 2013; Schultz, 2017) and the natural variability of precipitation. Despite of some newly emerging wine regions at extreme latitudes to the north (Jones and Schultz, 2016), Germany's winegrowing regions are still at the northern fringe of economically important grape cultivation of Europe. Historically,

https://doi.org/10.5194/esd-2021-9
Preprint. Discussion started: 31 March 2021

Earth System Dynamics Discussions

viticulture is practiced only in climatically favorable regions, mostly located along river valleys on slopes or lowlands in the southwest of Germany. In many of these areas viticulture is the main socio–economic factor, determining the cultural landscape with steep slope regions additionally forming biodiversity hotspots (Jäger and Porten, 2018; Petermann et al., 2012). Mean annual precipitation is generally low in these steep slope regions (500–770 mm; 1971–2000; Ahr, Mittelrhein, Mosel, Nahe, Rheingau; DWD (Deutscher Wetterdienst), 2020) and available water capacity (*AWC*) of soils is very heterogeneous, with the percentage of vineyards with low *AWC* being relatively high (example Rheingau region; *AWC* < 125 mm for nearly 50 % of steep slope areas; Löhnertz et al., 2004). In addition, the evaporative demand can vary substantially within a growing region, because of different slopes and aspects of the vineyard plots (Hofmann and Schultz, 2015). Therefore, risk assessment of climate driven changes in soil and plant water budget needs to be on a fine scale in order to identify possible adaptation measures within growing regions. These measures may span changes in the selection of grapevine varieties and rootstocks, soil, cover crop or canopy management up to the implementation of irrigation systems.

Predictions on a high spatial resolution are a challenge in climate impact studies and mainly limited by the size of one grid box of regional climate models (RCMs). Although climatic conditions within a grid box may change from being suitable for vineyards to areas unsuitable for the cultivation of grapevines, climate change impact studies for European viticulture where often forced to be performed based on the spatial resolution of the underlying gridded climate model data. Santos et al. (2012) analyzed observed shifts of bioclimatic indices (mainly temperature related) by means of the E–OBS gridded data set and the connection with large scale atmospheric forcing. Projections of bioclimatic indices based on RCMs were analyzed by Malheiro et al. (2010) and Fraga et al. (2013), the latter one also included possible changes in interannual variability. In terms of water supply, both studies projected a strong decrease of water availability for the Mediterranean basin but their projections differed for Central Europe ranging from a slight decrease (Fraga et al., 2013) to an increase (Malheiro et al., 2010). More specific regional aspects were analyzed by Santos et al. (2013) for the future of wine production in the Douro Valley (Portugal), and Moriondo et al. (2010) for expected changes for the premium wine quality area of Tuscany on a fine spatial resolution (1 km x 1 km, based on downscaling climate projections to station data and spatial interpolation). Only a few studies used data from soil maps including *AWC* as input data (Fraga et al., 2013; Moriondo et al., 2013), but on a spatial resolution still to coarse to represent the heterogeneity within growing regions. Recently, fine scale variability within growing regions were assessed and modelled within the ADVICLIM project but focusing only on temperature (Le Roux et al., 2017; Quénol et al., 2014).

Irrespective of weather conditions, the water balance of grapevines also depends on vineyard geometry (row distance, canopy height etc.), the training system (canopy shape), soil management practices and particularly site–specific factors such as *AWC*, slope and aspect (Hofmann and Schultz, 2015). These factors describe the interaction of vineyard site microclimate with water supply and atmospheric demand (Hoppmann et al., 2017; Sturman et al., 2017). Especially *AWC*, slope and aspect are very heterogeneous in steep slope regions and thus is the supply of and demand for water. Increasing water scarcity can put economic pressure on established growing regions, because severe drought stress causes losses of grape quality and yield. Adaptation measures like the implementation of irrigation systems are expensive and access to water in many places is restricted and difficult. Water withdrawal rights may also need to be adapted if water is taken from groundwater or surface water bodies. Since precipitation patterns are highly variable in space and time, it is problematic for growers and stakeholders to assess future developments and to make decisions for long–term mitigation and adaptation measures. Against this background, the identification of those vineyard plots or sites within growing regions likely exposed to an increasing risk for drought stress in the future can support the decision making process.

Therefore, the main objective of the study was to quantify the likelihood of risk for future water deficit on the spatial scale of individual vineyard plots within two German grape growing regions, Rheingau and Hessische Bergstraße. The scientific process included (i) statistical downscaling of an ensemble of climate models to the scale of station data, (ii) combining information from land registers, high–resolution soil maps and digital elevation models for the characterization of vineyard

https://doi.org/10.5194/esd-2021-9
Preprint. Discussion started: 31 March 2021

landscapes and their microclimate, (iii) performing vineyard water balance simulations driven by observed and simulated weather data for all vineyard plots.

2 Material and Methods

2.1 Study area, soil and climate conditions

The risk analysis was conducted for two out of the thirteen German winegrowing regions, the Rheingau and the Hessische Bergstraße, both located in the federal state of Hesse (Fig. 1). In the Rheingau, grapevines are cultivated on an area of 3191 ha (Destatis, 2018). The Rheingau is physiographically divided into the regions of upper and lower Rheingau (Löhnertz et al., 2004). The upper Rheingau includes an area of approx. 25 km length and 3–6 km width between Wiesbaden and Rüdesheim, bounded by the Rhine river to the south and the ridge of the Taunus mountain range in the north, and the vineyards near Hochheim on the Main river. Grapevines are cultivated between approx. 80–280 m altitude on a gently rolling hillscape. For most of the region, the soils developed from loess or sandy loess as parent material. They are fertile and have a balanced water budget. Soil erosion, intensified by agriculture over thousands of years, filled dells and in conjunction with soil formation by a variety of basement rocks (sand, clay, marl, limestone), led to the further differentiation of soils, where the loess layers were thin. The soils of the lower Rheingau in the west of Rüdesheim are very different. The direction of the Rhine changes towards north here into the Upper Middle Rhine Valley with its steep slopes. The parent material of the soil formation consists mainly of shallow glacial solifluction layers containing a lot of basement rock (sandstone, quartzite, slate). These soils are nutrient–poor, stony and shallow and generally have a low *AWC* (Löhnertz et al., 2004; Böhm et al., 2007). The second winegrowing region of Hesse, the Hessische Bergstraße, has a cultivated area of 462 ha (Destatis, 2018). The vineyards are located at the western slopes of the Odenwald mountain range, and at the eastern edge of the Upper Rhine Plain. Soils developed from loess are also dominating here. About 60 % of the soils are deep and rich with an *AWC* exceeding 200 mm, while about 20 % of the soils have an *AWC* below 125 mm, predominant at sites where the rooting depth is limited to 60–100 cm (Löhnertz et al., 2004).

The longest running weather station at Geisenheim (since 1884 in close proximity to the University and serviced by the Deutscher Wetterdienst, DWD, German Meteorological Service) had an average growing season temperature (AGST; Apr–Oct) for the reference period 1961–1990 of 14.5 °C and 548 mm annual precipitation. Spatial variation of temperature or precipitation within the region is relatively small. For a more recent period (2014-2018) and an array of weather stations (station specific temperature data for earlier or longer periods were only available for a limited number), AGST data ranged from 15.9 °C (station Frauenstein, elevation 151 m) to 16.9 °C (stations Ehrenfels, 101 m, and Erbach, 86 m) as compared to 16.3 °C for Geisenheim in the Rheingau and was 17.0 °C at the station Heppenheim (119 m) in the Hessische Bergstraße (see stations in Fig. 1). Annual precipitation (based on data available from 1959–1988 for various stations) varied from 545 mm (Geisenheim) to 636 mm in the Rheingau and from 750 mm to 824 mm in the Hessische Bergstraße and is almost evenly distributed over the year. Further details about precipitation characteristics are shown in Table 1.

2.2 Observed and synthetic weather series

In order to run the water balance model, transient daily data for temperature, solar radiation, relative humidity, wind speed and precipitation are required. Air temperature is used to model the development of grapevines and cover crops over annual cycles, and, together with solar radiation, wind speed and relative humidity, to calculate reference evapotranspiration (ET_0) according to Allen et al. (2005). We worked with four time series, two observed and two synthetic series.

https://doi.org/10.5194/esd-2021-9
Preprint. Discussion started: 31 March 2021


Earth System Dynamics Discussions

2.2.1 Observed weather data

The first observed series included daily weather data from 1959–1988 (the recording ended in 1989 at some of the stations) of 10 weather stations distributed across the regions (Fig. 1, Table 1) and were provided by the DWD (2018). All stations recorded precipitation and the station Bensheim additionally temperature and relative humidity (also used for the other stations at the Hessische Bergstraße). The station Geisenheim provided data for all five weather variables. More precisely, sunshine hours (SH) were measured here over the complete period providing a proxy for solar radiation (SR). A parallel measurement period of SR and SH at Geisenheim between 1981 and 1990 was used to establish correlation coefficients between these parameters (Hofmann et al., 2014) based on the Angstroem–Prescott equation and SR was calculated accordingly. Missing data or weather variables at other stations (wind speed and SR at the stations in the Hessische Bergstraße, all weather variables beside of precipitation at the stations in the Rheingau) were set equal to the data measured at Geisenheim. These data were used as model inputs for an assessment of the drought stress occurrence in the past as well as to calibrate the weather generator (see details below).

The second series included daily data from 2014–2018 and came from newly established weather stations (Fig. 1) by the University. These data were used for an assessment of observed drought stress in the recent past.

2.2.2 Synthetic data produced by a weather generator

Input weather series representing the baseline and future climate conditions were produced by the parametric stochastic weather generator (WG) M&Rfi, which is an improved follow–up version of Met&Roll generator (Dubrovský et al., 2000; Dubrovský et al., 2004). Met&Roll was based on the Wilks's (1992) version (adopted for use in future climate conditions) of the classical parametric generator developed by Richardson (1981). M&Rfi is a single–site multi–variate daily weather generator, in which the precipitation time series is modelled by a first–order Markov chain (occurrence of wet/dry days) and Gamma distribution (precipitation amount on wet days). The non–precipitation variables are simulated by a first–order autoregressive model whose parameters depend on wet/dry status of a given day. The M&Rfi generator has been used in many climate change impact experiments (e.g. Rötter et al., 2011; Hlavinka et al., 2015; Garofalo et al., 2018). This generator also participated in a complex validation experiment of the so–called VALUE project aiming at comparison of various downscaling approaches (Maraun et al., 2019; Gutiérrez et al., 2019). Two types of synthetic time series were produced by M&Rfi. The first time series representing the present (baseline) climate was used to validate the generator by comparing selected weather statistics derived from synthetic vs observed weather series, and the second one representing the future climate was used to assess changes of the drought stress occurrence for future climate change scenarios. In producing the first time series, WG parameters representing the statistical structure of the weather variability between 1959–1988 were derived from the observed station data (baseline climate), and then a 112–year synthetic series (1989–2100) representing the baseline climate (i.e. assuming no climate change) was produced by the WG. For the climate change scenarios (second series), we modified the WG parameters based on climate change scenarios derived from 10 future climate simulations made within the frame of the ENSEMBLES project (van der Linden and Mitchell, 2009; Table 2). Here, RCMs were used, which were driven by various Global Climate Models (GCMs) (Table 2) and run for the A1B emission scenario and approx. 25 km grid resolution. For each station and climate simulation, the data of the RCM grid boxes enclosing the weather stations were used to derive changes in WG parameters representing the RCM–based climate change scenario for 2058–2087. In order to construct transient time series consisting of observed data from 1961–1988 followed by synthetic weather data until 2100 (assuming a smooth increase in climate change signal), the WG parameters representing a given year Y were defined by modifying the WG parameters of the baseline climate with a climate change scenario, which was obtained by scaling the RCM–based scenario with a factor $k(Y)$, defined as

https://doi.org/10.5194/esd-2021-9
Preprint. Discussion started: 31 March 2021

Earth System Dynamics
Discussions
Open Access
EGU

$$k(Y) = \frac{T_G(Y;\mathrm{RCP8.5}) - T_G(1973;\mathrm{RCP8.5})}{T_G(2073;\mathrm{A1B}) - T_G(1975;\mathrm{A1B})}, \quad (1)$$

where T_G is the annual global mean temperature simulated by MAGICC(v.6) (Meinshausen et al., 2011). T_G(1973; RCP8.5), T_G(2073; A1B) and T_G(1975; A1B) refer to the centre years of the observed baseline (1959–1988), the RCM–future (2058–2087) and RCM–baseline (1961–1990) time slices, respectively, used to derive the WG parameters. MAGICC is a reduced–complexity climate model, which can simulate evolution of the annual global mean temperature for a chosen emission scenario and climate sensitivity. As we chose the high baseline emission scenario RCP8.5 (van Vuuren et al., 2011) for $T_G(Y)$ to calculate the factor $k(Y)$ in Eq. (1), the synthetic series representing the future climate were produced for RCP8.5.

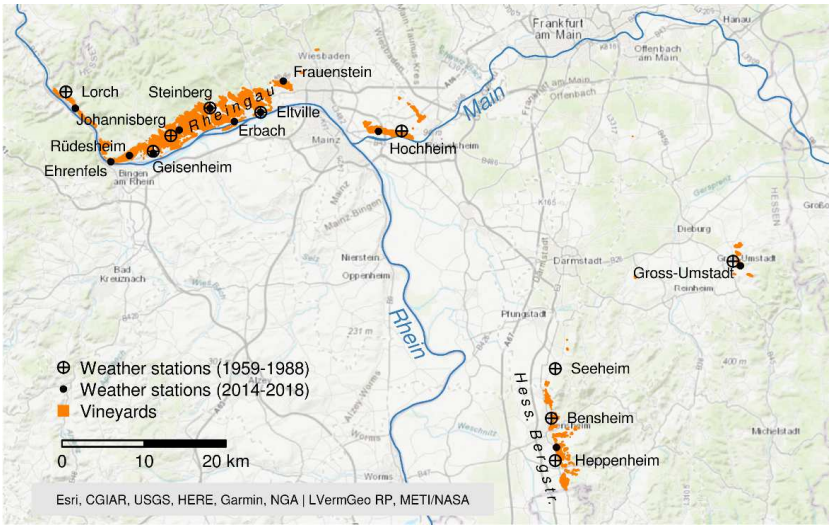

Figure 1: Map showing the winegrowing regions Rheingau and Hessische Bergstraße and the locations of weather stations (Source of the base map (modified): Esri, 2012).

Table 1: Description and parameters for precipitation (*P*) of the weather stations used to calibrate the weather generator with data from 1959–1988 and to analyse the drought stress occurrence of the past. Weather data were extracted from the database of the DWD (2018) and are available online at https://opendata.dwd.de.

Station	Station-ID	Region	Ele-vation (m)	Latitude	Longitude	Annual mean *P* 1959–1988 (mm)	Rainy days (days year^{-1})	*P*–intensity (mm rainy day^{-1})	Min. monthly *P* (month; mm)	Max. monthly *P* (month; mm)	Max. daily *P* 1959-1988 (mm)
Bensheim	355	Hess. Bergstr.	117	49.6961	8.6267	824	172	4.8	Feb; 49	Jun; 90	91
Heppenheim	2138	Hess. Bergstr.	101	49.6500	8.6333	806	170	4.8	Feb; 50	Jun; 88	70
Seeheim	4646	Hess. Bergstr.	132	49.7500	8.6333	770	149	5.2	Feb; 42	Jul; 86	65
Groß-Umstadt	1815	Hess. Bergstr.	168	49.8667	8.9333	750	157	4.8	Feb; 44	Jun; 82	95
Lorch	3062	Rheingau	90	50.0508	7.8064	604	164	3.7	Feb, 36	May; 65	76
Geisenheim	1580	Rheingau	118	49.9864	7.9542	545	168	3.2	Feb; 33	Jul; 58	55
Johannisberg	1581	Rheingau	177	50.0033	7.9836	602	159	3.9	Feb, 36	Jul; 64	61
Steinberg	1213	Rheingau	197	50.0333	8.0500	636	169	3.8	Feb, 39	Jul; 64	53
Eltville	1212	Rheingau	96	50.0286	8.1358	606	163	3.7	Feb, 35	Jul; 65	67
Hochheim	2242	Rheingau	115	50.0083	8.3738	586	171	3.4	Feb, 34	Aug; 63	77

https://doi.org/10.5194/esd-2021-9
Preprint. Discussion started: 31 March 2021

Earth System Dynamics Discussions

Table 2: Ensemble of climate models (van der Linden and Mitchell, 2009).

Institute	Climate–Simulation (RCM–GCM)
C4I	RCA3–HadCM3Q16
DMI	HIRHAM5–ARPEGE
DMI	HIRHAM5–ECHAM5
DMI	HIRHAM5–BCM
ETHZ	CLM–HadCM3Q0
KMNI	RACMO2–ECHAM5
MPI–M	REMO–ECHAM5
SMHI	RCA–BCM
SMHI	RCA–ECHAM5
SMHI	RCA–HadCM3Q3

2.3 The water balance model

We used the vineyard water balance model of Hofmann et al. (2014) which was developed and validated with the general growing and cultivation conditions of the study area presented here. This model accounts for different soil cultivation (bare soil, use of cover crops, or alternating use of both), and the impact of slope and aspect of the vineyard plots on received global radiation and ET_0. It includes a radiation partitioning model to separate ET_0 between grapevines and the soil based on Lebon et al. (2003) and accounts for different vineyard geometries. The development of the foliage of the grapevines and the cover crops is modelled based on temperature summations making it possible to run the model for multi–year applications. As heavy precipitation events are rare in the area of study, the original model did not account for surface runoff. To include possible changes of precipitation intensity in the future, the widely used curve number (CN) method (Cronshey et al., 1986; Woodward et al., 2003) was added to the original model. This procedure was developed for small watersheds taking into account that rainfall data are often only available in form of daily values and was tested in a vineyard soil water dynamics study (Gaudin et al., 2010). The curve numbers are available in form of tabled values and depend on the soil type, infiltration capacity of the soil and on the type of land use. We used CN = 86 for bare soil and CN = 58 for plant covered soils (Cronshey et al., 1986). Adjustments of the CN values depending on the antecedent moisture conditions before the wetting event were conducted as described in Maniak (2010). The impact of degree of slope on runoff was neglected, because several authors reported no clear findings (Emde, 1992, based on experiments on vineyards in the Rheingau area) or a small increase in runoff (Huang et al., 2006; Ebrahimian et al., 2012) within the range of the measurement accuracy of precipitation.

Since the individual geometry of each vineyard plot within the two regions was unknown, the calculations of radiation interception were performed for a uniform geometry representing a standard vertical shoot positioning system in Germany (Hoppmann et al., 2017). We used 2 m row distance, a foliage width of 0.4 m, a maximum row height of 2.10 m and minimum height of the lower end of the canopy of 0.8 m above the soil surface as base data. This is typical for the current and mid-term future situation, because more than 80 % of the new planted vineyards from 2002–2013 (> 30 % of the region) have a row distance of 180–200 cm (data from the EU vineyard register; RPDA, 2012).

For the simulations it was assumed that soil cultivation and cover crops in alternating rows are representative for the Rheingau and complete green cover (beside of a strip of 0.4 m underneath the vines) for the Hessische Bergstraße. This is currently typical for both regions.

https://doi.org/10.5194/esd-2021-9
Preprint. Discussion started: 31 March 2021

2.4 Soil data and spatial resolution

The study was based on the high spatial resolution of individual plots. The underlying data were provided in digital form as spatial polygons from the local authority in charge of the official EU vineyard register (RPDA, 2012). This resolution can be considered as high, with a total plot number of planted vineyards of 24858, with a mean area of 0.15 ha per plot. Plots up to 0.5 ha take up 79 % of total planted area with a maximum plot size of 4.2 ha. Each plot was linked with a digital elevation model at 1 m resolution to calculate the mean slope and aspect of the plots. The water balance model needs values for the available water capacity up to 2 m depth (AWC_{2m}) as the reservoir for grapevines, and 1 m depth (AWC_{1m}) as the reservoir for cover crops, and a value for the total evaporable water (*TEW*) of the soil surface layer, in order to calculate bare soil evaporation according to Allen (2011). The *TEW* is defined as the difference between the water content at field capacity and half of the water content at the permanent wilting point for the upper soil layer of 10–15 cm. The AWC_{2m}, AWC_{1m} were directly and the *TEW* indirectly obtained from a soil database of the official state map series BFD5W (HLNUG, 2008). To calculate the *TEW*, the BFD5W provides data on water, gravel and clay content for the plough horizon. We then used the methods described in Vorderbrügge et al. (2006) to estimate the water content at field capacity and the wilting point. The *TEW* was determined for the upper 10 cm soil layer in this study.

2.5 Assessment of drought stress

As an indicator to assess drought stress, we calculated the yearly sum of drought stress days during the vegetation period (1 May–30 September). A day was classified as drought stress day, if the remaining soil water content was smaller than 15 % AWC_{2m}. This approach is based on the assumption, that the AWC_{2m} of the soil maps corresponds to the total transpirable soil water (*TTSW*) used in earlier water balance studies (Lebon et al., 2003; Hofmann et al., 2014). The chosen threshold value of AWC_{2m} corresponds to the common plant physiological threshold value for severe stress of -0.6 MPa vine predawn leaf water potential (ψ_{pd}) as described in Hofmann et al. (2014).

3 Results

3.1 Validation of the weather generator

Downscaling data of climate models to station data is not trivial and all of the possible methods have pros and cons, which have to be considered in order to interpret the data and results (Maraun et al., 2010). Therefore, we tested the capability of the WG to reproduce the weather variables precipitation, solar radiation and the derived ET_0 over the annual cycle for the past (1959–1988). We additionally compared the interannual variability, in order to interpret the capacity to mimic the frequencies of simulated extreme dry or wet years. Figure 2 shows in the top row that annual cycles were well reproduced by the WG as compared to observed data (station Geisenheim as an example) and that no substantial bias of mean values or monthly sums between observed and synthetic values were apparent. The boxplots in the bottom row of Fig. 2 show on the other side that interannual variability is underestimated by the WG. This is especially the case for the simulated ET_0 and solar radiation in the range of the upper quartile of observed data, which are only partly (solar radiation) or not reproduced (ET_0) by the WG. Nevertheless, we assumed that this approach is suitable for long–term trends of climate simulations, but that frequencies especially for dry years will likely be underestimated by the WG. Data for other stations showed similar results. Additionally, observed differences of the weather variables between the weather stations for the past were quite consistently projected into the future by the WG, suggesting that climate simulations were feasible (data not shown).

https://doi.org/10.5194/esd-2021-9
Preprint. Discussion started: 31 March 2021

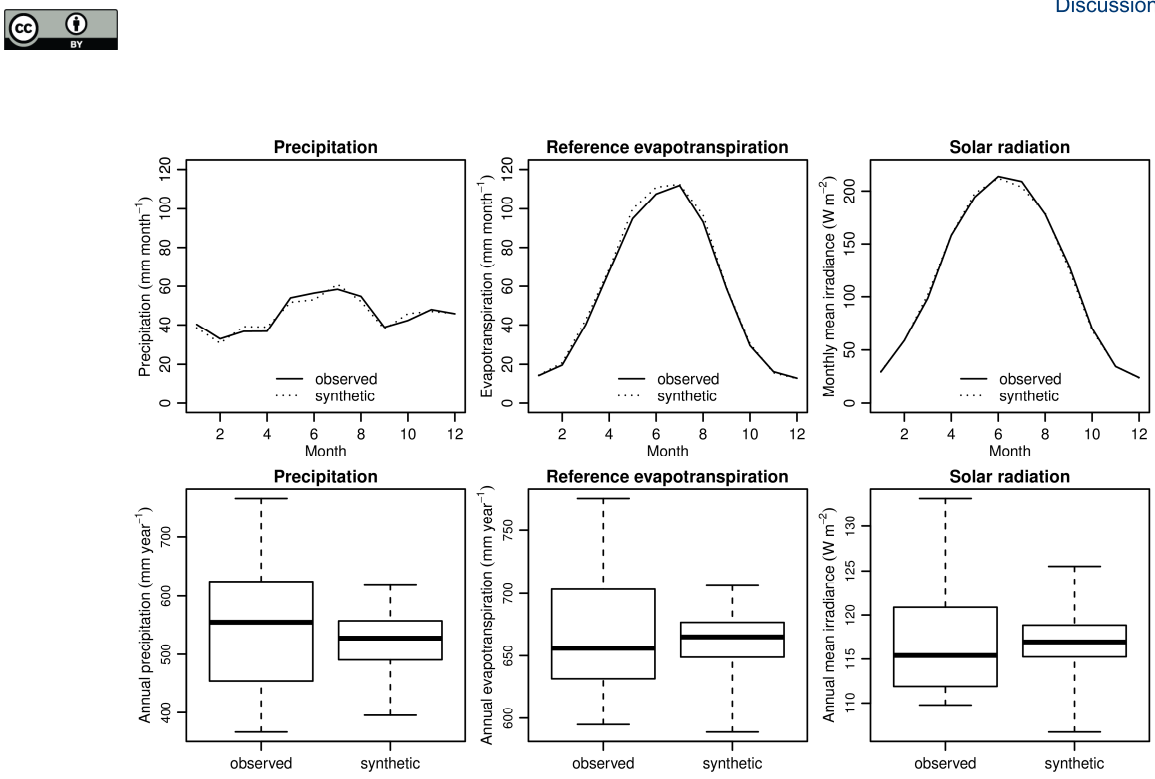

Figure 2: Comparison of 30 years of observed weather data (1959–1988, station Geisenheim, Rheingau, Germany) used to calibrate a weather generator (WG) and 30 years of synthetic weather simulated with the calibrated WG. Top row: Average annual patterns of precipitation, reference evapotranspiration and solar radiation in monthly resolution. Bottom row: Box plots of annual values (same 30–year periods as in the top row). The central box shows the interquartile range, the bold line the median; the whiskers extend to the extremes.

3.2 Water balance trends and drought stress occurrence based on observed weather data

3.2.1 Water balance

Figure 3 illustrates the trend and interannual variability of the water availability expressed as climatic water balance and calculated with data of the weather station Geisenheim. The climatic water balance represents the difference between the sum of precipitations and the sum of reference evapotranspiration over a hydrological year (1 Nov–31 Oct). The presentation of Fig. 3 does not directly allow conclusions on the extent of drought stress of a certain year, which additionally depends on site factors and the plant response to limit water use. Nevertheless, the climatic water balance has decreased by about 90 mm, if the two 30–year periods from 1959–1988 and 1989–2018 are compared. Additionally, the frequency of years with a climatic water balance lower than -200 mm has more than doubled over this period, from 8 to 18 years out of 30.

https://doi.org/10.5194/esd-2021-9
Preprint. Discussion started: 31 March 2021

Earth System Dynamics
Discussions
Open Access
EGU

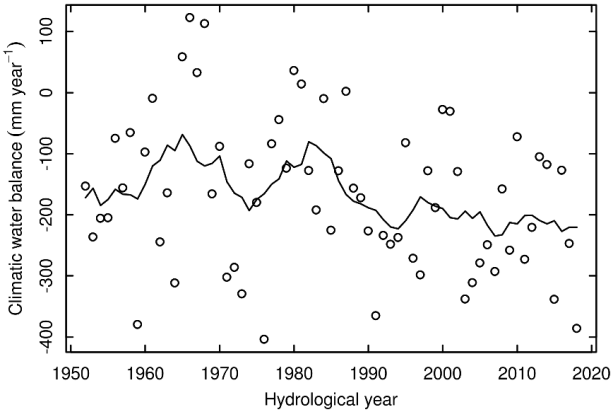

Figure 3: Climatic water balance, expressed as the difference between the sum of precipitations and the sum of reference evapotranspiration for a hydrological year (1 Nov–31 Oct) for the station Geisenheim (Rheingau), Germany. The solid line shows 11–year running mean values. The decreasing trend is significant ($p < 0.05$, Mann–Kendall trend test; calculated with the R–package Kendall; McLeod, 2011).

3.2.2 Drought stress simulations

Period 1959–1988: Water balance calculations for both growing regions with the data of the observation period from 1959–1988, showed that the five driest years were 1959, 1964, 1973, 1974 and 1976. In 1959 and 1976, this was related to hot and dry summers with many sunshine hours and high evaporative demand and in 1964, 1973 and 1974, because of extreme dry winters despite only average summers. On average, drought stress days were calculated in the range of 0–41 days per year and individual plot for the Rheingau and in the range of 0–23 days for the Hessische Bergstraße. The growing area affected by drought stress (the area with more than 10 calculated drought stress days per year on average) accounted for 6 % of the Rheingau (181 ha) and for only 1.2 % (5 ha) of the Hessische Bergstraße.

Period 2014–2018: Figure 4 shows the strong interannual variability of the soil water content dynamics for a typical vineyard (AWC_{2m} = 110 mm, south oriented, 27.5° slope) in the steep slopes of the lower Rheingau area in the west of Rüdesheim (Fig. 1). In 2014 and 2017 moderate drought stress occurred after mid–June (after flowering) until the beginning (2014), respectively the end of July (2017), followed by moderate (2017) to wet conditions during the ripening period. The year 2018 started with a well–refilled soil profile after winter and was quite wet until mid–June, after which an extreme dry and hot period followed, leading to a fast reduction in soil water content and severe drought stress.

The map in Fig. 5 shows the simulated spatial distribution of the sum of drought stress days for the entire Rheingau region for the year 2018 based on data of the weather station network (Fig. 1). The year 2018 had the highest sum of annual ET_0 (876 mm) since 1951 (first year where all weather variables to calculate ET_0 were recorded at the station Geisenheim). The simulations agreed with observations in the lower Rheingau (near 7.9°E and 49.98°N, Fig. 4, and between 60 to 92 days (ψ_{pd}) < -0.6 MPa), where for many vineyards strong reductions in quantity and restricted sugar accumulation were observed. In that particular vintage, the growing area with more than 10 calculated drought stress days was 13 % (400 ha).

https://doi.org/10.5194/esd-2021-9
Preprint. Discussion started: 31 March 2021

Earth System Dynamics
Discussions
Open Access
EGU

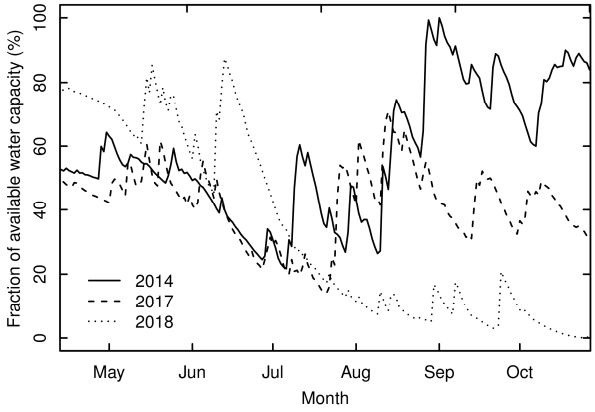

Figure 4: Seasonal patterns of the fraction of available water capacity (AWC_{2m}) for a typical steep slope vineyard in the west of the Rheingau area (near station Ehrenfels, see map in Fig. 1). Simulations were conducted with a water balance model for the years 2014, 2017 and 2018. Parameters for the model input were: AWC_{2m} = 110 mm, south oriented, 27.5° slope, 2 m row distance, one row bare soil, one row cover crop.

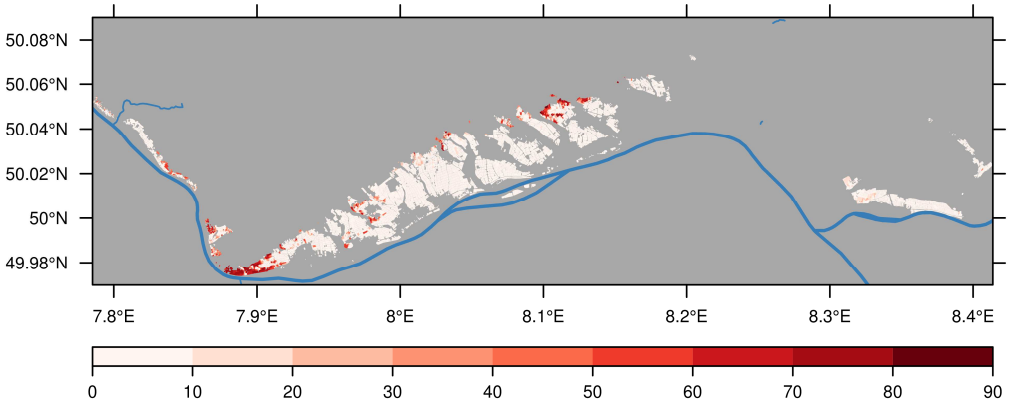

Figure 5: Number of simulated drought stress days per vineyard plot for the winegrowing region Rheingau, Germany, during the 2018 vegetation period (1 May–30 Sep). Calculations were conducted with a water balance model based on data from weather stations and a digital soil map on the assumption of alternating soil cultivation (one row bare soil, one row cover crop).

3.3 Water balance trends and drought stress occurrence based on climate simulations

3.3.1 Projected annual trends of precipitation and the climatic water balance to 2100

Annual precipitation projected by the ensemble of climate simulations for the station Geisenheim showed a high bandwidth (Fig. 6a). The change signal (difference of mean values between the time–period 2071–2100 and the period of observed values 1961–1988) ranged from a decrease of -141 and -53 mm to an increase of +73 and +170 mm for the two most extreme simulations. For seven simulations, the projected trends were significant after the year 2073 (Mann–Kendall trend test, $p < 0.05$, Fig. 6b). The bandwidth of change signal for the climatic water balance per hydrological year (1 Nov–31 Oct) was stronger and ranged from -257 mm and -182 mm to +67 mm and +169 mm (Fig. 7a). The statistical significance of the trends was comparable to the trends of precipitation (Fig. 7b). This additional increase of the bandwidth results from the ensemble change signals of annual ET_0 from +3 mm to +207 mm (data not shown). It should be noted that simulation results with CLM–HadCM3Q0 showed, contrasting to all other models, a strong increase in global radiation of 10 % until 2100, resulting in a strong increase of ET_0 and thus a strong reduction in climatic water balance until the end of the century (Fig. 7a). All other simulations projected a decrease of global radiation up to -15 % until 2100 (data not shown).

https://doi.org/10.5194/esd-2021-9
Preprint. Discussion started: 31 March 2021

Earth System Dynamics
Discussions
Open Access
EGU

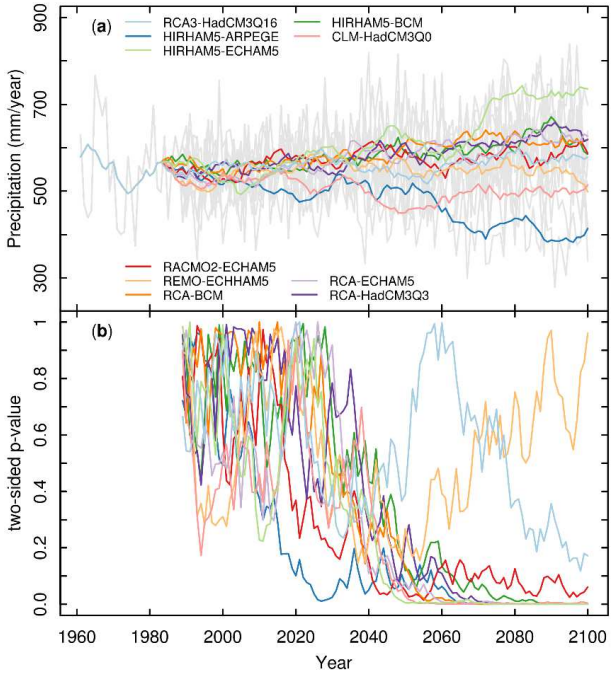

Figure 6: (a) Annual precipitation rates of 10 climate simulations with different models for the station Geisenheim (Rheingau), Germany. Grey lines show the range of annual values of all models, coloured lines 11–year running means for individual model runs. The period from 1961–1988 shows observed data. (b) p–values calculated with Mann–Kendall trend test for time series of annual precipitation rates shown in (a) starting in 1961.

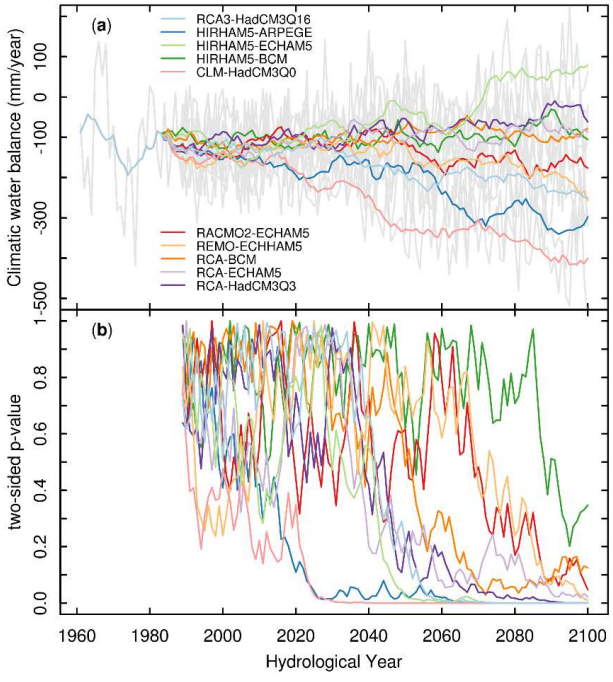

Figure 7: (a) Climatic water balance of 10 climate simulations of different models for the station Geisenheim (Rheingau), Germany, per hydrological year (1 Nov–31 Oct). Grey lines show the range of annual values of all models, coloured lines 11–year running means for individual model runs. The period from 1961–1988 shows observed data. (b) p–values calculated with Mann–Kendall trend test for time series shown in (a) starting in 1961.

https://doi.org/10.5194/esd-2021-9
Preprint. Discussion started: 31 March 2021

Earth System Dynamics Discussions
Open Access
EGU

3.3.2 Projected seasonal trends (spring, summer, autumn, winter) of precipitation and the climatic water balance to 2100

Seasonal trends of the model ensemble are shown in Fig. 8. In part, the results of precipitation change signals (2071–2100 compared to 1961–1988, Table 3) reflected possible future seasonal shifts. The bandwidth of change signals of the transition seasons spring (March, April, May (MAM); -17 to +58 mm, Fig. 8a) and autumn (September, October, November (SON); -28 to +42 mm, Fig. 8c) is quite high, whereby in both seasons some models projected no changes of precipitation in the future up to 2100. In winter (December, January, February (DJF), Fig. 8c) all models except one (-14 mm) projected a precipitation increase (+23 to +41 mm). In summer (June, July, August (JJA), Fig. 8b), the ensemble splits up in three groups at the end of the century, one model projects an increase of precipitation (+39 mm), six models are in the range of a small decrease to no change (-22 to +1 mm) and three models project a precipitation decrease (-60 to -81 mm). In general, this indicates an increase of precipitation in winter possibly connected with a decrease of precipitation in a future summer.

Taking into account reference evapotranspiration by calculating the seasonal climatic water balance, the picture changed towards dryer conditions (Fig. 9, Table 3). In winter, the plus of precipitation is slightly reduced due to higher ET_0 (-21 to +34 mm, Fig. 9d). This is relevant in water balance calculations, because (actual) evapotranspiration is normally not reduced by dry soils due to the better water availability during these months. This also applies in parts for spring (-42 to +62 mm, Fig. 9a) and autumn (-51 to +32 mm, Fig. 9c). A clear change signal could be identified for summer, only one model projected an increase (+48 mm) all others a decrease in the range of -191 to -17 mm (Fig. 9b) due to a significant change signal for ET_0 in the range of -9 to +130 mm (Table 3). Climate simulations for other weather stations showed similar results.

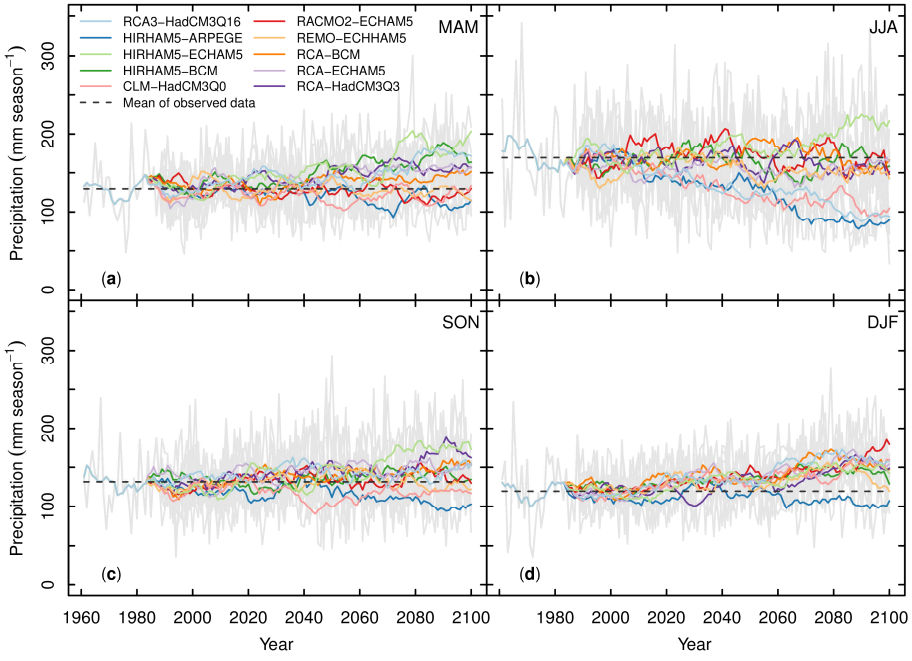

Figure 8: Seasonal precipitation simulated with 10 climate models for the station Geisenheim (Rheingau), Germany. Grey lines show the range of annual values of all models, coloured lines 11–year running means for individual model runs. The period from 1961–1988 represents observed data and the dashed baselines illustrate their mean values. (a) MAM, spring, March, April, May; (b) JJA, summer, June, July, August; (c) SON, autumn, September, October, November; (d) DJF, winter, December, January, February.

https://doi.org/10.5194/esd-2021-9
Preprint. Discussion started: 31 March 2021

Earth System Dynamics
Discussions
Open Access
EGU

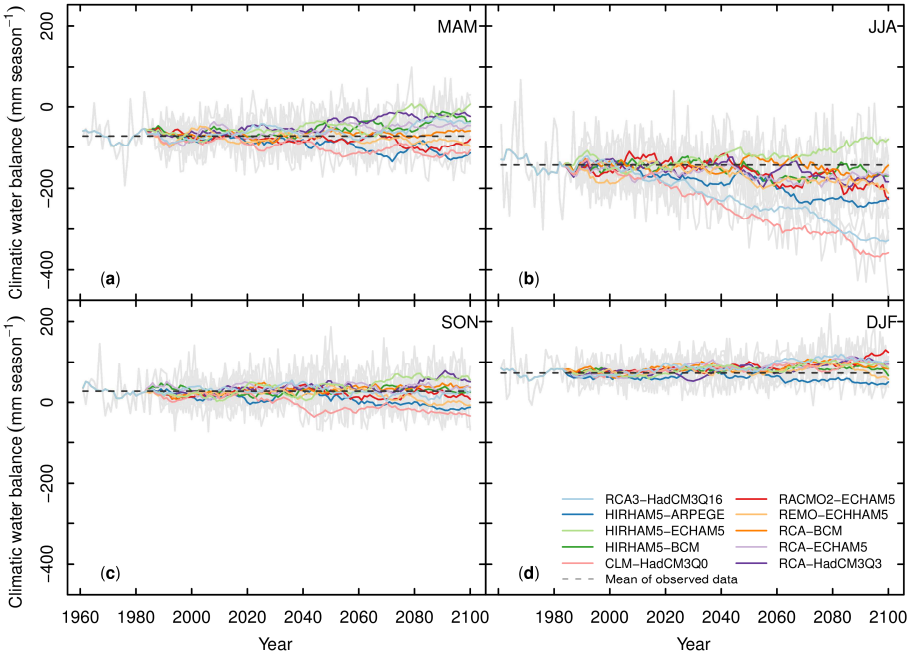

Figure 9: Seasonal climatic water balance simulated with 10 climate models for the station Geisenheim (Rheingau), Germany. Grey lines show the range of annual values of all models, coloured lines 11–year running means for individual model runs. The period from 1961–1988 represents observed data and the dashed baselines illustrate their mean values. (a) MAM, spring, March, April, May; (b) JJA, summer, June, July, August; (c) SON, autumn, September, October, November; (d) DJF, winter, December, January, February.

Table 3: Bandwidth of change signals of 10 climate simulations with different models for the station Geisenheim (Rheingau), Germany. For precipitation (*P*), reference evapotranspiration (ET_0) and climatic water balance (*CWB*, P-ET_0) for spring (March, April, May, MAM), summer (June, July, August, JJA), autumn (September, October, November, SON) and winter (December, January, February, DJF), change signals were calculated by the difference of the individual model means between the time–period 2071–2100 and the observation period 1961–1988.

Season	**Ensemble change signal (2071–2100 minus 1961–1988)**		
	P (mm)	ET_0 (mm)	*CWB* (mm)
Spring (MAM)	-17 to +58	-23 to +32	-42 to +62
Summer (JJA)	-81 to +39	-9 to +130	-191 to +48
Autumn (SON)	-28 to +42	+6 to +36	-51 to +32
Winter (DJF)	-14 to +41	+6 to +18	-21 to +34
Year	-141 to +170	+3 to +207	-260 to +166

3.3.3 Projected drought stress risk for the winegrowing regions Rheingau and Hessische Bergstraße

As most of the climate simulations showed significant annual precipitation trends in the second half of the century (Fig. 6b) and indicated changes in climatic water balance, we calculated the average number of drought stress days for the time–periods 1989–2018 and 2041–2070 for each vineyard plot and climate model. Based on this calculation, two indices were derived. The first one is describing the overall grape–growing surface area affected by drought stress, defined as the sum of the area of all individual vineyard plots with on average per time–period ten or more days of drought stress during the vegetation period. The second one is the drought stress change signal, calculated as the difference of the average number of drought stress days per vineyard plot and climate simulation between both time–periods. The calculation of the grape–growing surface area showed that three models for both regions projected a substantial increase of the potential drought stress area, possibly affecting 10 to 30 % (Rheingau), respectively 16–20 % (Hessische Bergstraße), of the growing–area with drought stress for the future period

https://doi.org/10.5194/esd-2021-9
Preprint. Discussion started: 31 March 2021

Earth System Dynamics Discussions
Open Access
EGU

2041–2070. For both regions, the median of the climate model ensemble of the drought stress area increased slightly by 2 % and reflected projected changes in the range of no change to a small increase of the ensemble, while one model projected a decrease of 2 % for the period 2041–2070 compared to 1989–2018 (Fig. 10).

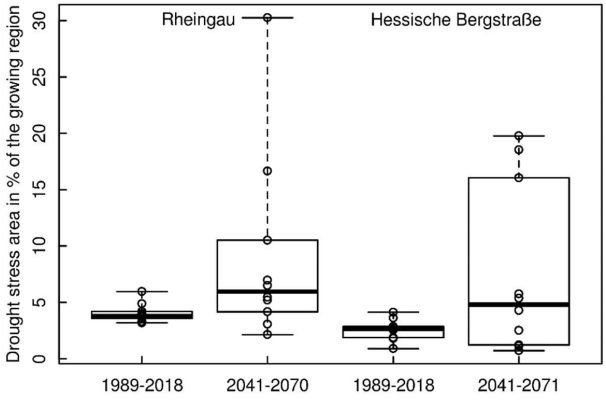

Figure 10: Potential drought stress area of two winegrowing regions (Rheingau and Hessische Bergstraße) in Germany for two time–periods (1989–2018 and 2041–2070), calculated with a water balance model, soil maps and 10 climate simulations with different models. A vineyard plot was allocated to the drought stress affected area, if on average 10 or more days with drought stress during the vegetation period (1 May–30 Sep) were calculated. Individual model results are shown as points in the boxplots.

The calculation of the drought stress change signals per vineyard plot allowed the creation of maps, to illustrate spatially the impact of the projected climate trends. The maps for the "dry" and for the "wet" simulation at the extremes and the simulation close to the median of the ensemble (Fig. 10) are shown in Fig. 11 (Rheingau) and Fig. 12 (Hessische Bergstraße). In case of the dry simulation (Fig. 11a), the vineyards where drought stress already occurred in the past (in the lower Rheingau, and near Johannisberg 50.0 °N, 7.97 °E, see Fig. 1; and Martinsthal 50.05 °N, 8.12 °E, not indicated on Fig. 1) would be affected in parts (lower Rheingau) by a strong increase of drought stress. But drought stress could also increase on plots where it is at present unknown, around the two weather stations with the lowest annual rainfall, Geisenheim and Hochheim (Table 1), although many of those plots have a good *AWC* (> 175 mm; Löhnertz et al., 2004). The moderate simulation close to the median of the ensemble (Fig. 10) projected a drought stress increase up to 20 days in the Rheingau but confined to vineyard plots already affected by drought stress in 1989–2018 (Fig. 11b). In case of the "wet" simulation a moderate (but not complete) decrease of drought stress is projected, but only on plots where it occurred in the past (Fig. 11c). At the Hessische Bergstraße, the dry simulation would affect vineyards distributed over the whole region, but with a weaker change signal compared to the Rheingau (Fig. 12a). In case of the simulation close to the median, only a few plots were affected by a drought stress increase of up to 11 days (Fig. 12b). Changes for the wet simulation were negligible (Fig. 12c).

https://doi.org/10.5194/esd-2021-9
Preprint. Discussion started: 31 March 2021

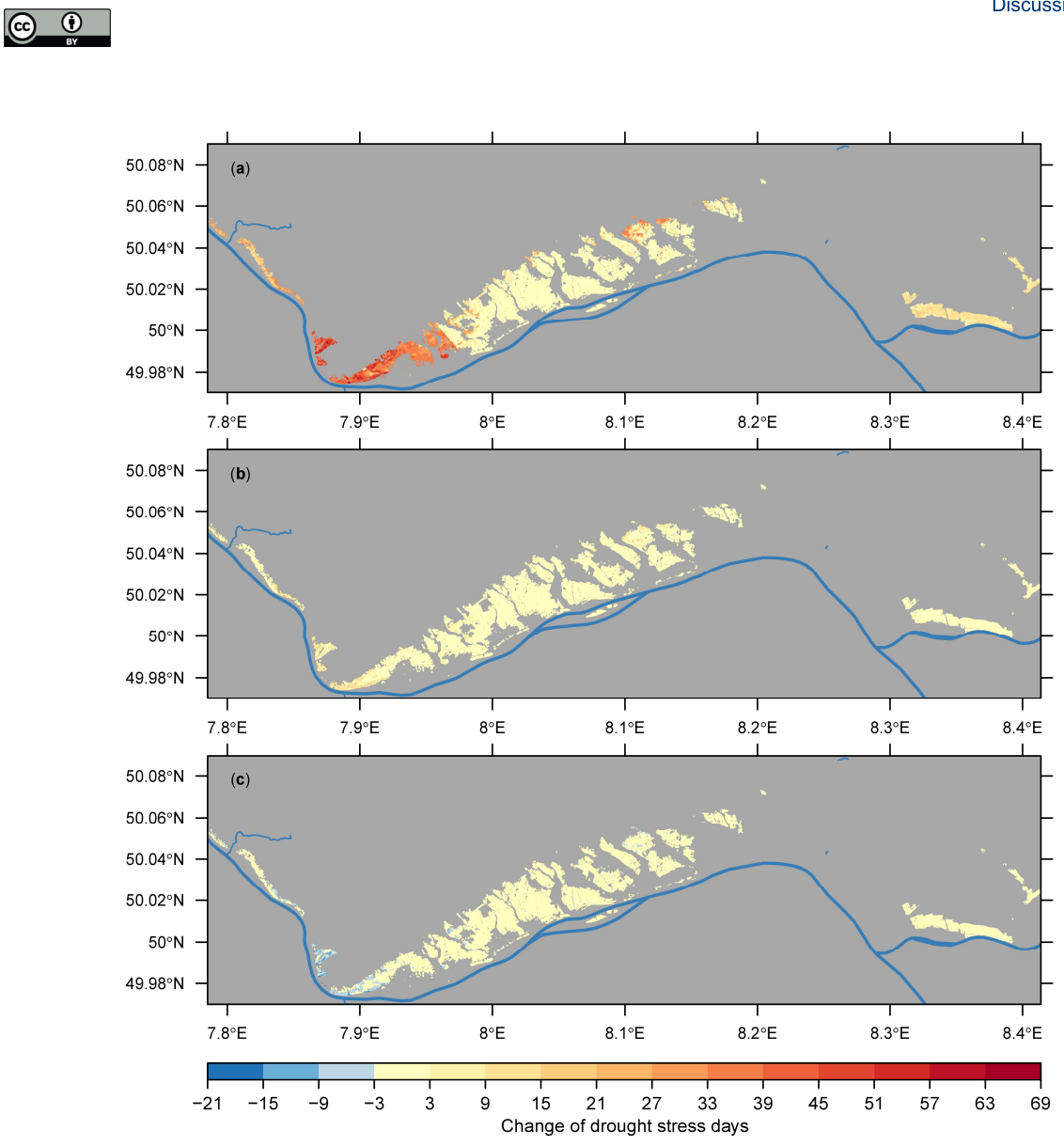

Figure 11: Projected change of the occurrence of drought stress days for the growing region Rheingau, calculated with a water balance model on the assumption of alternating soil cultivation (one row bare soil, one row cover crop). The maps show the difference between the number of the mean drought stress days per vegetation period (1 May–30 Sep) and individual plot for the periods 2041–2070 minus 1989–2018. (a) Results of the climate simulation calculating the strongest increase, (b) the simulation close to the ensemble median, and (c) the simulation projecting the strongest decrease of the drought stress area of an ensemble of 10 climate models.

https://doi.org/10.5194/esd-2021-9
Preprint. Discussion started: 31 March 2021

Earth System Dynamics
Discussions
Open Access
EGU

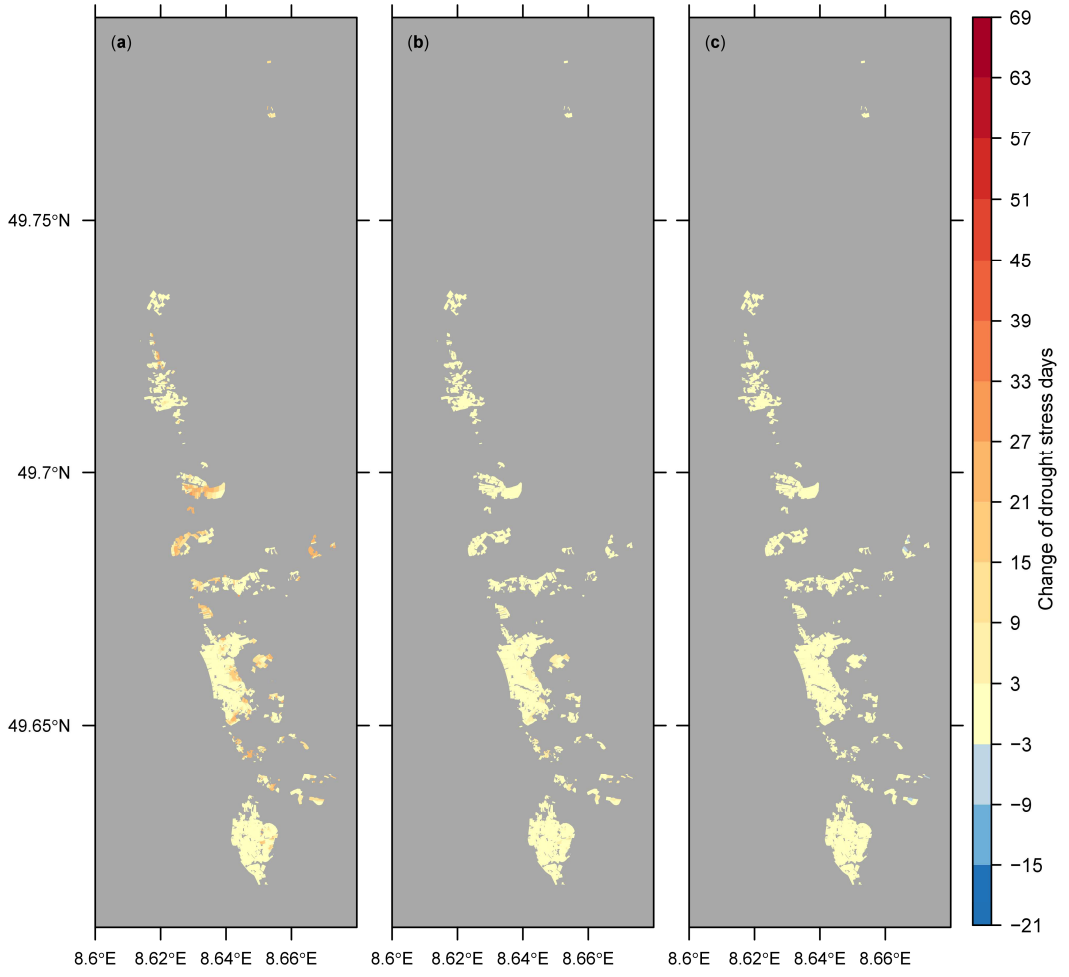

Figure 12: Projected change of the occurrence of drought stress days for the growing region Hessische Bergstraße, Germany, calculated with a water balance model on the assumption of cover crop use in every row. The maps show the difference between the number of the mean drought stress days per vegetation period (1 May–30 Sep) and individual plot for the periods 2041–2070 minus 1989–2018. (a) Results of the climate simulation calculating the strongest increase, (b) the simulation close to the ensemble median, and (c) the simulation projecting the strongest decrease of the drought stress area of an ensemble of 10 climate models.

4 Discussion

4.1 Global and regionals aspects of the uncertainty of the projections

Climate projections and impact analyses are subject to a number of uncertainties. In the understanding of climate change, these uncertainties are in general related to the uncertain future external forcing by greenhouse gas emissions, the impact of external forcing factors on climate and the degree of natural variability of the climate system (Kjellström et al., 2011). In impact-analyses, methodical imperfections of the impact models result in further uncertainties. This study looked on a comparably small region, thus the ability of the RCMs to reproduce spatial weather patterns is one additional source of uncertainty. The water balance model itself or previous versions have been validated with field observations on different vineyard plots of the current study area as well as other regions and in different climates (Lebon et al., 2003; Pellegrino et al., 2006). Yet, on a regional scale, it requires high quality soil data, which have a strong influence on the result of the calculations as a possible source of error. The soil data go back mainly to soil mappings conducted from 1947–1958 (Böhm et al., 2007), where at distances of 20 m x 20 m, respectively 25 m x 25 m, soil samples down to 2 m depth were taken and analyses performed. Since

https://doi.org/10.5194/esd-2021-9
Preprint. Discussion started: 31 March 2021

then, based on land consolidation projects, and individual interventions in parts of the complete landscape, some attributes might have changed in local spots, but in general, the soil maps are still describing the current situation quite well as demonstrated in a follow–up study (Zimmer, 1999).

To capture the magnitude of uncertainties related to possible future climate evolution for the selected emission scenario, we used climate projections for the period 2058–2087 simulated by ten climate models of the ENSEMBLES project. These data were used to derive the climate change scenario, which was further scaled by smoothly increasing change in global mean temperature (as projected by the MAGICC model for the selected RCP8.5 emission scenario) and used to modify the weather generator parameters, in order to produce transient time series for several weather stations. The simulations of the precipitation data showed a high bandwidth at the end of the century. This bandwidth is comparable with the results of the REKLIES–DE project (±20 % for annual precipitation, region Germany and drainage basins of large rivers, 2070–2099 compared to 1971–2000), calculated with 37 climate simulations including the EURO–CORDEX data (Hübener et al., 2017; Bülow et al., 2019). Additionally, similar seasonal shifts (increase of winter and decrease of summer precipitations) were reported in this study. This bandwidth could be reduced if the extreme models at the upper or lower edge would be excluded, but since no direct model flaws were detected, this would exclude possible future climate realisations. Furthermore, climate models cannot be considered as fully independent from each other (Kreienkamp et al., 2012; Flato et al., 2013), which rules out the conclusion that if the majority of results from model runs point into one direction, that this would automatically mean a higher probability for this climate realisation. However, diverging databases bear uncertainties in risk assessment and decision support processes. Noteworthy, the projected bandwidth for precipitation for the mitigation scenario RCP2.6 are less than half of those for RCP8.5 (Hübener et al., 2017).

Impact modellers are currently confronted with a large number of climate models and bias correction and downscaling methods (Maraun et al., 2015) and choosing of appropriate methods depends on the relevant question and is currently also among viticulture scientists under debate (Quénol et al., 2017). We decided to use station (point) data, because of the existence of quality–controlled observed data in good spatial resolution and the overall knowledge of the correlation between weather data inside of vineyards and the grapevines response to different weather patterns. Additionally, the impact model was validated with measured weather and field data. In order to downscale from the spatial means of grid box data of the RCMs to the spatial scale of station data, we used a weather generator to produce point data on the same scale as the weather stations and to simulate small–scale weather patterns. One water budget simulation driven by the climate models predicted that drought stress would be less problematic in the future. This would not be expected from observations in the recent past, where drought stress occurrence has increased. The decrease in the climatic water balance is related to an increase in ET_0, because for the Rheingau region (station Geisenheim) no seasonal trend in precipitation rates is noticeable for the past. The observed increase of ET_0 is a combined effect of an increase in global radiation and temperature. Changes in wind velocity, as observed in other regions on the globe, can be excluded (Schultz, 2017). The data extracted from the weather station clearly show the effect of global dimming (after World War II to the 1980ies) and brightening (since then) periods (Wild, 2009; Hofmann and Schultz, 2010) related to a period of strong pollution (dimming) and cleaning of the atmosphere (brightening) and observed in many places on Earth. This is reflected in an increase in mean solar irradiance from 117 W m^{-2} for the period from 1951–1989 to 130 W m^{-2} for the period from 1990–2018 (station Geisenheim). Furthermore, the most intensive droughts for the two growing regions in the years 2003 and 2018 were related to heat waves with high ET_0 values. Heat wave frequencies on a global scale have increased in the past (Schär et al., 2004) and are predicted to increase further in the near feature, irrespective of the emission scenario (Coumou and Robinson, 2013). A study of Kornhuber et al. (2019) found that the weather extremes of the early summer 2018, where heat and rainfall extremes were recorded in the mid–latitudes of the northern hemisphere, were connected with a persistent wave pattern in the Jetstream, which was also observed during the European heat waves of 2003, 2006 and 2015. In addition, the number of such wave patterns has increased significantly during the last two decades. Since we downscaled the grid box means of climate models to station (point) data in order to reduce the bias, but with the shortcoming

https://doi.org/10.5194/esd-2021-9
Preprint. Discussion started: 31 March 2021


Earth System Dynamics Discussions

of reduced interannual variability, it is likely that frequencies of such extreme years are underestimated (Fig. 2). As expected, the reduced interannual variability compared to station data was also found in grid box data of RCMs of the region, because these data represent spatial means. Fraga et al. (2013) reported an increase of interannual variability of the temperature based Huglin–Index and the precipitation/evapotranspiration based dryness–index for many parts of Europe including the study region, by comparing the period from 2041–2070 with 1961–2000, calculated with 16 climate simulations from the ENSEMBLES project. On the other side, the frequency of such extreme years is the main cause for growers to think about cost intensive adaptation measures like irrigation (Santos et al., 2020). The impact analysis for perennial crops, not only grapevines, could profit enormously from climate simulations with the feature of well–reproduced interannual variability.

Despite of the reduced interannual variability, the climate projections showed seasonal shifts. The impact of seasonality of precipitation on grape quality is not fully understood (Sadras et al., 2012b). Dry conditions during the ripening period and harvest are in general positive for fruit quality and health, but severe drought stress can lead to a cessation of sugar accumulation, as observed in specific plots of the study area during the 2018 and 2019 vintages. Seasonal shifts of precipitation could reduce the impact of dry spells on plots with sufficient capacity to store available water, by enhanced refilling in winter. Trömel and Schönwiese (2007) reported that the trends for the probability for observed monthly extreme precipitation in Germany varied substantial on a spatial scale and also projected near future changes of extreme precipitation showed heterogeneous spatial change patterns in summer (Feldmann et al., 2013). The performance of many downscaling and bias correction methods to represent temporal aspects of the climate has become only recently a topic of research (Maraun et al., 2019).

4.2. Impact Model shortcomings with respect to projected atmospheric CO_2 concentrations

The water balance model currently does not account for the impact of increasing CO_2 on stomatal conductance (g_s) and transpiration. Xu et al. (2016) reported that the stomatal response to elevated CO_2 depended greatly on environmental variables and species and referred to studies where double ambient CO_2 decreased g_s by 40–50 %. A general survey of the response of stomatal aperture to an increase to 560 µmol mol^{-1} in CO_2–concentration (from 380 µmol mol^{-1}; Ainsworth and Rogers, 2007) across a variety of plant species showed an approximate reduction of about 20 %. Experiments of field grown grapevines under elevated CO_2 showed no uniform results and ranged from an observed decrease of stomatal conductance (Everard et al., 2017) to no significant changes (Bindi et al., 2001; Moutinho–Pereira et al., 2009) to even an increase (Wohlfahrt et al., 2018). A simple, but physically based approach to assess the impact of reduced g_s on ET_0 is provided by the equations of Allen et al. (1998). In the Penman–Monteith equation, the bulk surface resistance for water transport is the variable depending on stomatal conductance/resistance (Lovelli et al., 2010). Applied to the weather data of the year 2017 of Geisenheim, a reduction of stomatal conductance of 20 % would lead to a reduction of 3 % of the annual sum of ET_0 (from 723 to 702 mm $year^{-1}$). Therefore, in the assessment of drought, the possible reduction of transpiration caused by elevated CO_2 is likely not the key point but there is currently a lack of knowledge about the impact of elevated CO_2 on the physiology of grapevines in combination with drought stress under field conditions. Additionally, depending on the grapevine cultivar, the responses to water deficit can be quite diverse (Schultz, 1996, 2003; Costa et al., 2012; Bota et al., 2016).

4.3 Possible impacts on grape quality and cultivation caused by moderate drought stress scenarios

Most of the models showed a small increase of the number of drought stress days in the range of 5–20 days for vineyards of the lower Rheingau and small parts of the upper Rheingau, in general on plots where drought stress occurred already in the recent past. From these simulations, some sub –regions with an increased future risk for drought stress could be identified. For already irrigated plots, the scenario outcomes mean that growers would have to irrigate between one to three times more per season on average. The used threshold value, to classify a day as a drought stress day (ψ_{pd} < -0.6 MPA) represents relative severe drought stress with a strong decrease of assimilation rate (Schultz and Lebon, 2005) and cessation of vegetative growth

https://doi.org/10.5194/esd-2021-9
Preprint. Discussion started: 31 March 2021


Earth System Dynamics Discussions

(Van Leeuwen et al., 2017). The viticultural impact of drought stress depends also on the phenological stage when it occurs and the duration of such events. Before flowering (beginning of June –mid June), even moderate drought stress (-0.6 MPA < ψ_{pd} < -0.2 MPa) is possibly negative, because it can reduce cluster size and berry numbers (Keller, 2005). Matthews et al. (1987) reported that early drought stress (before fruit softening, i.e. about beginning of August to mid-August in the Rheingau area) had a stronger impact on yield than late drought stress. Early drought stress also has a stronger impact on the final berry size (Ojeda et al., 2001). In the context of the majority of models predicting a decrease in climatic water balance in JJA (Fig. 9b) this would indicate a likely future yield effect. Impacts on quality components aside of primary compounds like sugar and acids are much more difficult to predict, vary between white and red varieties (Sadras et al., 2012b; Savoi et al., 2016) and depend on complex interactions with many environmental factors difficult to completely assess for in climate change studies (Van Leeuwen et al., 2017; Santos et al., 2020).

4.4 Adaptation measures with respect to the local environment

The simulations showed a widespread array of possible changes making it difficult to generalize adaptation strategies. Both viticultural regions are located in areas where nitrate leaching to the groundwater is a severe environmental issue (Löhnertz et al., 2004). This threat would certainly be enhanced in the future because of higher mineralization rates, caused by increasing temperature (both air and soil) and rainfall in winter (Table 3). The use of cover crops or natural vegetation to cover the soil on the complete vineyard surface area during the winter months is the most important measure to counteract this development (Berthold et al., 2016). Similarly, these measures and possibly reduced tillage are also important for the summer months to protect against leaching and erosion. Against this background, the choice of rootstock and/or the flexibility of irrigation systems might be the best choice, if it is feasible for the latter to bring water to the vineyards. Due to increased temperature combined with relatively unchanged but still highly variable precipitation patterns (Fig. 8c), the occurrence of warm and wet conditions during the ripening period (September, October) has increased the risk for rot (Schultz and Hofmann, 2015). Vineyards with low available water capacity are in general more susceptible to variable precipitation, because the soil water potential changes much faster per unit of stored soil water imposing large fluctuations on plant water status.

5 Conclusions

Based on an ensemble of climate model simulations, a water balance model, a digital soil map, an elevation model and a land register, our study provides a risk assessment with respect to the future occurrence of drought stress, applied to individual vineyard plots of two winegrowing regions. The bandwidth of the results ranged from a small decrease (one simulation) to a moderate increase of drought stress (median of the ensemble), predominantly on plots already temporarily affected by water deficit, up to a drought stress occurrence touching 20–30 % of the growing regions. As drought stress is already currently observed in steep slope vineyards with shallow soils, these sub–regions were identified as future risk areas by most of the simulations. The results illustrate the large heterogeneity of the water supply within growing regions and between neighbouring vineyards and the need to improve high resolution modelling approaches. Mid– and long–term adaptation measures need to respect local conditions and will necessitate individual, precision–farming–like application of cultivation practices. In combination with weather station networks delivering real time data, the presented framework may also serve as a decision support tool to growers and consultants in the future.

Data availability. Observed weather data of the DWD can be found at https://opendata.dwd.de/ and weather data of the Hochschule Geisenheim University at http://rebschutz.hs-geisenheim.de/wetterstationen/tagesauswertung.php. Outputs from the weather generator simulations are available on request to the corresponding author.

https://doi.org/10.5194/esd-2021-9
Preprint. Discussion started: 31 March 2021

Author Contributions. MH and HS developed the concept and research goals, DM, MD, CV, and MH designed the methodology, CV downloaded and processed the future climate change scenarios, MD programmed and calibrated the weather generator, MH ran the water balance simulations, prepared the original draft and produced all figures, all authors contributed to writing, review and editing.

Competing interests. The authors declare that they have no conflict of interest.

Acknowledgments. This research was funded by the Hessian Agency for Nature Conservation, Environment and Geology (HLNUG) as a part of the INKLIM–A project. We thank Klaus Friedrich, Matthias Schmanke (HLNUG) and Christoph Presser (Regierungspräsidium Darmstadt, RPD) for combining the comprehensive databases of vineyard plots, elevation and soil maps. We thank Heike Hübener (HLNUG) for fruitful discussions about how to perform climate change impact studies on individual vineyards.

References

Ainsworth, E. A., and Rogers, A.: The response of photosynthesis and stomatal conductance to rising [CO_2]: mechanisms and environmental interactions, Plant, Cell & Environment, 30, 258-270, 10.1111/j.1365-3040.2007.01641.x, 2007.

Allen, R. G.: Skin layer evaporation to account for small precipitation events—An enhancement to the FAO-56 evaporation model, Agricultural Water Management, 99, 8-18, 10.1016/j.agwat.2011.08.008, 2011.

Allen, R. G., Pereira, L. S., Raes, D., and Smith, M.: Crop evapotranspiration- Guidelines for computing crop water requirements - FAO Irrigation and drainage paper 56, FAO Irrigation and Drainage Papers, FAO - Food and Agriculture Organization of the United Nations, Rome, 1998.

Allen, R. G., Walter, I. A., Elliot, R., Howell, T., Itenfisu, D., and Jensen, M.: The ASCE Standardized Reference Evapotranspiration Equation, ASCE-EWRI Task Committee Report, 2005.

Berthold, G., Meilinger, F., Dettweiler, I., and Muskat, S.: Die Umsetzung der Wasserrahmenrichtlinie in Hessen - Ausblick und Rückblick, in: Umweltschonender Weinbau - das solidarische Ziel, Hessisches Ministerium für Umwelt, Klimaschutz, Landwirtschaft und Verbraucherschutz, 2016.

Bindi, M., Fibbi, L., and Miglietta, F.: Free Air CO_2 Enrichment (FACE) of grapevine (*Vitis vinifera* L.): II. Growth and quality of grape and wine in response to elevated CO_2 concentrations, European Journal of Agronomy, 14, 145-155, 10.1016/S1161-0301(00)00093-9, 2001.

Böhm, P., Friedrich, K., and Sabel, K.-J.: Die Weinbergsböden von Hessen, Hessisches Landesamt für Umwelt und Geologie, Wiesbaden, 2007.

Bormann, H.: Sensitivity analysis of 18 different potential evapotranspiration models to observed climatic change at German climate stations, Climatic Change, 104, 729-753, 10.1007/s10584-010-9869-7, 2011.

Bota, J., Tomás, M., Flexas, J., Medrano, H., and Escalona, J. M.: Differences among grapevine cultivars in their stomatal behavior and water use efficiency under progressive water stress, Agricultural Water Management, 164, 91-99, 10.1016/j.agwat.2015.07.016, 2016.

Bülow, K., Huebener, H., Keuler, K., Menz, C., Pfeifer, S., Ramthun, H., Spekat, A., Steger, C., Teichmann, C., and Warrach-Sagi, K.: User tailored results of a regional climate model ensemble to plan adaption to the changing climate in Germany, Adv. Sci. Res., 16, 241-249, 10.5194/asr-16-241-2019, 2019.

Costa, J. M., Ortuño, M. F., Lopes, C. M., and Chaves, M. M.: Grapevine varieties exhibiting differences in stomatal response to water deficit, Functional Plant Biology, 39, 179-189, 10.1071/FP11156, 2012.

https://doi.org/10.5194/esd-2021-9
Preprint. Discussion started: 31 March 2021

Coumou, D., and Robinson, A.: Historic and future increase in the global land area affected by monthly heat extremes, Environmental Research Letters, 8, 034018, 10.1088/1748-9326/8/3/034018, 2013.

Cronshey, R., McCuen, R. H., Miller, N., Rawls, W., Robbins, S., and Woodward, D.: Urban Hydrology for Small Watersheds TR-55, United States Department of Agriculture – NRCS, 1986.

Destatis: Landwirtschaftliche Bodennutzung -Rebflächen-, Statistisches Bundesamt, Wiesbaden, 2018.

Dubrovský, M., Žalud, Z., and Šťastná, M.: Sensitivity of Ceres-Maize Yields to Statistical Structure of Daily Weather Series, Climatic Change, 46, 447-472, 10.1023/A:1005681809065, 2000.

Dubrovský, M., Buchtele, J., and Žalud, Z.: High-Frequency and Low-Frequency Variability in Stochastic Daily Weather Generator and Its Effect on Agricultural and Hydrologic Modelling, Climatic Change, 63, 145-179, 10.1023/b:clim.0000018504.99914.60, 2004.

DWD Climate Data Center (CDC): Historical daily station observations (temperature, pressure, precipitation, sunshine duration, etc.) for Germany, version v006, https://opendata.dwd.de, 2018.

DWD Climate Data Center (CDC): Multi-annual station means for the climate normal reference period 1971-2000, for current station location and for reference station location, Version V0.x, https://opendata.dwd.de, 2020

Ebrahimian, M., Nuruddin, A. A. B., Soom, M., Sood, A. M., and Neng, L. J.: Runoff Estimation in Steep Slope Watershed with Standard and Slope-Adjusted Curve Number Methods, Pol. J. Environ. Stud., 21, 1191-1202, 2012.

Emde, K.: Experimentelle Untersuchungen zu Oberflächenabfluß und Bodenaustrag in Verbindung mit Starkregen bei verschiedenen Bewirtschaftungssystemen in Weinbergsarealen des oberen Rheingaus, Geisenheimer Berichte, 12, Gesellschaft zur Förderung der Forschungsanstalt Geisenheim, Geisenheim, 1992.

Erfurt, M., Skiadaresis, G., Tijdeman, E., Blauhut, V., Bauhus, J., Glaser, R., Schwarz, J., Tegel, W., and Stahl, K.: A multidisciplinary drought catalogue for southwestern Germany dating back to 1801, Nat. Hazards Earth Syst. Sci., 20, 2979-2995, 10.5194/nhess-20-2979-2020, 2020.

Esri: "Topographic" [base map]. Scale not specified. "Worldwide Topographic Map". 19. February 2012. http://www.arcgis.com/home/item.html?id=30e5fe3149c34df1ba922e6f5bbf808f. (25. May 2017). 2012.

Everard, J. E., Dale, U., Rachel, K., and Michael, T.: Multi-seasonal effects of warming and elevated CO_2 on the physiology, growth and production of mature, field grown, Shiraz grapevines, OENO One, 51, 127-132, 10.20870/oeno-one.2017.51.2.1586, 2017.

Feldmann, H., Schädler, G., Panitz, H.-J., and Kottmeier, C.: Near future changes of extreme precipitation over complex terrain in Central Europe derived from high resolution RCM ensemble simulations, International Journal of Climatology, 33, 1964-1977, 10.1002/joc.3564, 2013.

Flato, G., Marotzke, J., Abiodun, B., Braconnot, P., Chou, S. C., Collins, W., Cox, P., Driouech, F., Emori, S., Eyring, V., Forest, C., Gleckler, P., Guilyardi, E., Jakob, C., Kattsov, V., Reason, C., and Rummukainen, M.: Evaluation of Climate Models, in: Climate Change 2013: The Physical Science Basis. Contribution of Working Group I to the Fifth Assessment Report of the Intergovernmental Panel on Climate Change, edited by: Stocker, T. F., Qin, D., Plattner, G.-K., Tignor, M., Allen, S. K., Boschung, J., Nauels, A., Xia, Y., Bex, V., and Midgley, P. M., Cambridge University Press, Cambridge, United Kingdom and New York, NY, USA, 741-866, 2013.

Fraga, H., Malheiro, A. C., Moutinho-Pereira, J., and Santos, J. A.: Future scenarios for viticultural zoning in Europe: ensemble projections and uncertainties, International journal of biometeorology, 57, 909-925, 10.1007/s00484-012-0617-8, 2013.

Garofalo, P., Ventrella, D., Kersebaum, K. C., Gobin, A., Trnka, M., Giglio, L., Dubrovský, M., and Castellini, M.: Water footprint of winter wheat under climate change: Trends and uncertainties associated to the ensemble of crop models, Science of The Total Environment, 658, 1186-1208, https://doi.org/10.1016/j.scitotenv.2018.12.279, 2019.

https://doi.org/10.5194/esd-2021-9
Preprint. Discussion started: 31 March 2021

Gaudillère, J. P., Van Leeuwen, C., and Ollat, N.: Carbon isotope composition of sugars in grapevine, an integrated indicator of vineyard water status, Journal of Experimental Botany, 53, 757-763, 10.1093/jexbot/53.369.757, 2002.

Gaudin, R., Celette, F., and Gary, C.: Contribution of runoff to incomplete off season soil water refilling in a Mediterranean vineyard, Agricultural Water Management, 97, 1534-1540, 10.1016/j.agwat.2010.05.007, 2010.

Gruber, B.: Untersuchungen zur Bodenfeuchtedynamik und zum Pflanzenwasserhaushalt bei verschiedenen Bodenmanagement- und Laubwandsystemen von *Vitis vinifera* L. (cv. Riesling) im Steilhang - ein Ansatz zur bedarfsgerechten Steuerung von Tröpfchenbewässerungsanlagen, Geisenheimer Berichte, 71, Gesellschaft zur Förderung der Hochschule Geisenheim e.V., 235 pp., 2012.

Gruber, B. R., and Schultz, H. R.: Coupling of plant to soil water status at different vineyard sites, Acta Hort. (ISHS), 689, 381-390, 2005.

Gutiérrez, J. M., Maraun, D., Widmann, M., Huth, R., Hertig, E., Benestad, R., Roessler, O., Wibig, J., Wilcke, R., Kotlarski, S., San Martín, D., Herrera, S., Bedia, J., Casanueva, A., Manzanas, R., Iturbide, M., Vrac, M., Dubrovsky, M., Ribalaygua, J., Pórtoles, J., Räty, O., Räisänen, J., Hingray, B., Raynaud, D., Casado, M. J., Ramos, P., Zerenner, T., Turco, M., Bosshard, T., Štěpánek, P., Bartholy, J., Pongracz, R., Keller, D. E., Fischer, A. M., Cardoso, R. M., Soares, P. M. M., Czernecki, B., and Pagé, C.: An intercomparison of a large ensemble of statistical downscaling methods over Europe: Results from the VALUE perfect predictor cross-validation experiment, International Journal of Climatology, 39, 3750-3785, 10.1002/joc.5462, 2019.

Hanel, M., Rakovec, O., Markonis, Y., Máca, P., Samaniego, L., Kyselý, J., and Kumar, R.: Revisiting the recent European droughts from a long-term perspective, Scientific Reports, 8, 9499, 10.1038/s41598-018-27464-4, 2018.

Hlavinka, P., Kersebaum, K. C., Dubrovský, M., Fischer, M., Pohanková, E., Balek, J., alud, Z., and Trnka, M.: Water balance, drought stress and yields for rainfed field crop rotations under present and future conditions in the Czech Republic, Climate Research, 65, 175-192, 10.3354/cr01339, 2015.

Hartmann, D. L., Klein Tank, A. M. G., Rusticucci, M., Alexander, L. V., Brönnimann, S., Charabi, Y., Dentener, F. J., Dlugokencky, E. J., Easterling, D. R., Kaplan, A., Soden, B. J., Thorne, P. W., Wild, M., and Zhai, P. M.: Observations: Atmosphere and Surface, in: Climate Change 2013: The Physical Science Basis. Contribution of Working Group I to the Fifth Assessement Report of the Intergovernmental Panel on Climate Change, Cambridge University Press, Cambridge, United Kingdom and New York, NY, USA, 2013.

HLNUG: Bodenflächendaten weinbauliche Nutzfläche 1:5000 BFD5W, Hessisches Landesamt für Naturschutz, Umwelt und Geologie, Wiesbaden, 2008.

Hofmann, M., and Schultz, H. R.: Warum es seit 1989 wieder heller wird, Der Deutsche Weinbau, 16-17, 32-34, 2010.

Hofmann, M., Lux, R., and Schultz, H. R.: Constructing a framework for risk analyses of climate change effects on the water budget of differently sloped vineyards with a numeric simulation using the Monte Carlo method coupled to a water balance model, Frontiers in Plant Science, 5, 1-22, 10.3389/fpls.2014.00645, 2014.

Hofmann, M., and Schultz, H. R.: Modeling the water balance of sloped vineyards under various climate change scenarios, BIO Web of Conferences, 5, 01026, 10.1051/bioconf/20150501026, 2015.

Hoppmann, D., Schaller, K., and Stoll, M.: Terroir, Ulmer Verlag, Stuttgart, 372 pp., 2017.

Huang, M., Gallichand, J., Wang, Z., and Goulet, M.: A modification to the Soil Conservation Service curve number method for steep slopes in the Loess Plateau of China, Hydrological Processes, 20, 579-589, 10.1002/hyp.5925, 2006.

Hübener, H., Bülow, K., Fooken, C., Früh, B., Hoffmann, P., Höpp, S., Keuler, K., Menz, C., Mohr, V., Radtke, K., Ramthun, H., Spekat, A., Steger, C., Toussaint, F., Warrach-Sagi, K., and Woldt, M.: ReKliEs-De Ergebnisbericht, 10.2312/WDCC/ReKliEsDe_Ergebnisbericht, 2017.

Jäger, L., and Porten, M.: Biodiversität in Weinbausteillagen, Die Winzer-Zeitschrift, 3, 26-28, 2018.

https://doi.org/10.5194/esd-2021-9
Preprint. Discussion started: 31 March 2021

Jones, G. V., Duchène, E., Tomasi, D., Yuste, J., Bratislavska, O., Schultz, H. R., Martinez, C., Boso, S., Langellier, F., Perruchot, C., and Guimberteau, G.: Changes in European Winegrape Phenology and Relationships with Climate, XIV International GESCO-Viticulture-Congress, Geisenheim, 2005b, 55-61, 2005a.

Jones, G. V., White, M., Cooper, O., and Storchmann, K.: Climate Change and Global Wine Quality, Climatic Change, 73, 319-343, 10.1007/s10584-005-4704-2, 2005b.

Jones, G. V., and Schultz, H. R.: Climate change and emerging cool climate wine regions, Wine & Viticulture Journal, November/December, 51-53, 2016.

Keller, M.: Deficit Irrigation and Vine Mineral Nutrition, Am J Enol Viticult, 56, 267-283, 2005.

Kenny, G. J., and Harrison, H. A.: The Effects of Climate Variability and Change on Grape Suitability in Europe, Journal of Wine Research, 3, 163-183, 1992.

Kjellström, E., Nikulin, G., Hansson, U., Strandberg, G., and Ullerstig, A.: 21st century changes in the European climate: uncertainties derived from an ensemble of regional climate model simulations, Tellus A: Dynamic Meteorology and Oceanography, 63, 24-40, 10.1111/j.1600-0870.2010.00475.x, 2011.

Kornhuber, K., Osprey, S., Coumou, D., Petri, S., Petoukhov, V., Rahmstorf, S., and Gray, L.: Extreme weather events in early summer 2018 connected by a recurrent hemispheric wave-7 pattern, Environmental Research Letters, 14, 054002, 10.1088/1748-9326/ab13bf, 2019.

Kreienkamp, F., Huebener, H., Linke, C., and Spekat, A.: Good practice for the usage of climate model simulation results - a discussion paper, Environmental Systems Research, 1, 1-13, 10.1186/2193-2697-1-9, 2012.

Le Roux, R., de Rességuier, L., Corpetti, T., Jégou, N., Madelin, M., van Leeuwen, C., and Quénol, H.: Comparison of two fine scale spatial models for mapping temperatures inside winegrowing areas, Agricultural and Forest Meteorology, 247, 159-169, 10.1016/j.agrformet.2017.07.020, 2017.

Lebon, E., Dumas, V., Pieri, P., and Schultz, H. R.: Modelling the seasonal dynamics of the soil water balance of vineyards, Functional Plant Biology, 30, 699-710, doi:10.1071/FP02222, 2003.

Löhnertz, O., Hoppmann, D., Emde, K., Friedrich, K., Schmanke, M., and Zimmer, T.: Die Standortkartierung der hessischen Weinbaugebiete, Geologische Abhandlungen Hessen, 114, edited by: Becker, R. E., Hessisches Landesamt für Umwelt und Geologie, Wiesbaden, 2004.

Lovelli, S., Perniola, M., Di Tommaso, T., Ventrella, D., Moriondo, M., and Amato, M.: Effects of rising atmospheric CO_2 on crop evapotranspiration in a Mediterranean area, Agricultural Water Management, 97, 1287-1292, 10.1016/j.agwat.2010.03.005, 2010.

Malheiro, A. C., Santos, J. A., Fraga, H., and Pinto, J. G.: Climate change scenarios applied to viticultural zoning in Europe, Climate Research, 43, 163-177, 10.3354/cr00918, 2010.

Maniak, U.: Hydrologie und Wasserwirtschaft, Springer-Verlag, Berlin Heidelberg, 2010.

Maraun, D., Wetterhall, F., Ireson, A. M., Chandler, R. E., Kendon, E. J., Widmann, M., Brienen, S., Rust, H. W., Sauter, T., Themeßl, M., Venema, V. K. C., Chun, K. P., Goodess, C. M., Jones, R. G., Onof, C., Vrac, M., and Thiele-Eich, I.: Precipitation downscaling under climate change: Recent developments to bridge the gap between dynamical models and the end user, Rev. Geophys., 48, RG3003, 10.1029/2009rg000314, 2010.

Maraun, D., Widmann, M., Gutiérrez, J. M., Kotlarski, S., Chandler, R. E., Hertig, E., Wibig, J., Huth, R., and Wilcke, R. A. I.: VALUE: A framework to validate downscaling approaches for climate change studies, Earth's Future, 3, 1-14, https://doi.org/10.1002/2014EF000259, 2015.

Maraun, D., Huth, R., Gutiérrez, J. M., Martín, D. S., Dubrovsky, M., Fischer, A., Hertig, E., Soares, P. M. M., Bartholy, J., Pongrácz, R., Widmann, M., Casado, M. J., Ramos, P., and Bedia, J.: The VALUE perfect predictor experiment: Evaluation of temporal variability, International Journal of Climatology, 39, 3786-3818, 10.1002/joc.5222, 2019.

https://doi.org/10.5194/esd-2021-9
Preprint. Discussion started: 31 March 2021

Matthews, M. A., Anderson, M. M., and Schultz, H. R.: Phenologic and growth responses to early and late season water deficits in Cabernet franc, Vitis, 26, 147-160, 1987.

McLeod, A. I.: Kendall: Kendall rank correlation and Mann-Kendall trend test. R package version 2.2. http://CRAN.R-project.org/package=Kendall, 2011.

Meinshausen, M., Raper, S. C. B., and Wigley, T. M. L.: Emulating coupled atmosphere-ocean and carbon cycle models with a simpler model, MAGICC6 – Part 1: Model description and calibration, Atmos. Chem. Phys., 11, 1417-1456, 10.5194/acp-11-1417-2011, 2011.

Moriondo, M., Bindi, M., Fagarazzi, C., Ferrise, R., and Trombi, G.: Framework for high-resolution climate change impact assessment on grapevines at a regional scale, Regional Environmental Change, 11, 553-567, 10.1007/s10113-010-0171-z, 2010.

Moriondo, M., Jones, G. V., Bois, B., Dibari, C., Ferrise, R., Trombi, G., and Bindi, M.: Projected shifts of wine regions in response to climate change, Climatic Change, 119, 825-839, 10.1007/s10584-013-0739-y, 2013.

Morlat, R., Penavayre, M., Jacquet, A., Asselin, C., and Lemaitre, C.: Influence des terroirs sur le fonctionnement hydrique et al photosynthèse de la vigne en millessime exceptionnellement sec (1990). Conséquence sur la maturation du raisin, International Journal of Vine and Wine Sciences, 26, 197-218, 1992.

Moutinho-Pereira, J., Goncalves, B., Bacelar, E., Boaventura Cunha, J., Coutinho, J., and Correira, C. M.: Effects of elevated CO_2 on grapevine (*Vitis vinifera* L.): Physiological an yield attributes, Vitis, 48, 159-165, 2009.

Ojeda, H., Deloire, A., and Carbonneau, A.: Influence of water deficits on grape berry growth, Vitis, 40, 141-145, 2001.

Pellegrino, A., Gozé, E., Lebon, E., and Wery, J.: A model-based diagnosis tool to evaluate the water stress experienced by grapevine in field sites, European Journal of Agronomy, 25, 49-59, 10.1016/j.eja.2006.03.003, 2006.

Petermann, J., Petersen, B., and Gnittke, I.: Hotspots im Bundesprogramm biologische Vielfalt, Referat Öffentlichkeitsarbeit, Bundesministerium für Umwelt, Naturschutz und Reaktorsicherheit (BMU), 2012.

Quénol, H., Grosset, M., Barbeau, G., van Leeuwen, C., Hofmann, M., Foss, C., Irimia, L., Rochard, J., Boulanger, J.-P., Tissot, C., and Miranda, C.: Adaptation of Viticulture to Climate Change: High Resolution Observations of Adaptation scenario for Viticulture: The ADVICLIM European Project, Bulletin de l´OIV, 87, 395-406, 2014.

Quénol, H., Garcia de Cortazar Atauri, I., Bois, B., Sturman, A., Bonnardot, V., and Le Roux, R.: Which climatic modeling to assess climate change impacts on vineyards?, OENO One, 51, 91-97, 10.20870/oeno-one.2016.0.0.1869, 2017.

Richardson, C. W.: Stochastic simulation of daily precipitation, temperature, and solar radiation, Water Resources Research, 17, 182-190, 10.1029/WR017i001p00182, 1981.

Rötter, R. P., Palosuo, T., Pirttioja, N. K., Dubrovsky, M., Salo, T., Fronzek, S., Aikasalo, R., Trnka, M., Ristolainen, A., and Carter, T. R.: What would happen to barley production in Finland if global warming exceeded 4°C? A model-based assessment, European Journal of Agronomy, 35, 205-214, 10.1016/j.eja.2011.06.003, 2011.

RPDA: Die Weinbaukartei des Landes Hessen - Stand 2012, Regierungspräsidium Darmstadt - Dezernat Weinbau, Eltville, Darmstadt, 2012.

Sadras, V. O., Montoro, A., Moran, M. A., and Aphalo, P. J.: Elevated temperature altered the reaction norms of stomatal conductance in field-grown grapevine, Agricultural and Forest Meteorology, 165, 35-42, 10.1016/j.agrformet.2012.06.005, 2012a.

Sadras, V. O., Schultz, H. R., Girona, J., and Marsal, J.: Grapevine, in: Crop yield response to water - FAO irrigation and drainage paper 66, edited by: Steduto, P., Hsiao, T. C., Fereres, E., and Raes, D., Food and Agriculture Organization of the United Nations, Rome, 460-485, 2012b.

Santos, J. A., Malheiro, A. C., Pinto, J. G., and Jones, G. V.: Macroclimate and viticultural zoning in Europe: observed trends and atmospheric forcing, Climate Research, 51, 89-103, 10.3354/cr01056, 2012.

https://doi.org/10.5194/esd-2021-9
Preprint. Discussion started: 31 March 2021

Santos, J. A., Grätsch, S. D., Karremann, M. K., Jones, G. V., and Pinto, J. G.: Ensemble projections for wine production in the Douro Valley of Portugal, Climatic Change, 117, 211-225, 10.1007/s10584-012-0538-x, 2013.

Santos, J. A., Fraga, H., Malheiro, A. C., Moutinho-Pereira, J., Dinis, L.-T., Correia, C., Moriondo, M., Leolini, L., Dibari, C., Costafreda-Aumedes, S., Kartschall, T., Menz, C., Molitor, D., Junk, J., Beyer, M., and Schultz, H. R.: A Review of the Potential Climate Change Impacts and Adaptation Options for European Viticulture, Applied Sciences, 10, 3092, 10.3390/app10093092, 2020.

Savoi, S., Wong, D. C. J., Arapitsas, P., Miculan, M., Bucchetti, B., Peterlunger, E., Fait, A., Mattivi, F., and Castellarin, S. D.: Transcriptome and metabolite profiling reveals that prolonged drought modulates the phenylpropanoid and terpenoid pathway in white grapes (*Vitis vinifera* L.), BMC Plant Biol., 16, 67, 10.1186/s12870-016-0760-1, 2016.

Schär, C., Vidale, P. L., Luthi, D., Frei, C., Haberli, C., Liniger, M. A., and Appenzeller, C.: The role of increasing temperature variability in European summer heatwaves, Nature, 427, 332-336, 10.1038/nature02300, 2004.

Schultz, H. R.: Water relations and photosynthetic responses of two grapevine cultivars of different geographical origin during water stress, Acta Horticulturae, 427, 251-266, 1996.

Schultz, H. R.: Climate Change and viticulture: A European perspective on climatology, carbon dioxide and UV-B effects, Australian Journal of Grape and Wine Research, 6, 2-12, 2000.

Schultz, H. R.: Differences in hydraulic architecture account for near-isohydric and anisohydric behaviour of two field-grown *Vitis vinifera* L. cultivars during drought, Plant, Cell & Environment, 26, 1393-1405, 10.1046/j.1365-3040.2003.01064.x, 2003.

Schultz, H. R.: Issues to be considered for strategic adaptation to climate evolution – is atmospheric evaporative demand changing?, OENO One, 51, 109-114, 10.20870/oeno-one.2017.51.2.1619, 2017.

Schultz, H. R., and Lebon, E.: Modelling the effect of climate change on grapevine water relations, Acta Hort. (ISHS), 689, 71-78, 2005.

Schultz, H. R., and Jones, G. V.: Climate Induced Historic and Future Changes in Viticulture, Journal of Wine Research, 21, 137 - 145, 2010.

Schultz, H. R., and Hofmann, M.: The ups and downs of environmental impact on grapevines: future challenges in temperate viticulture, in: Grapevine in a Changing Environment: A Molecular and Ecophysiological Perspective, edited by: Gerós, H., Chaves, M. M., Medrano, H., and Delrot, S., Wiley-Blackwell, 2015.

Sturman, A., Zawar-Reza, P., Soltanzadeh, I., Katurji, M., Bonnardot, V., Parker, A. K., Trought, M. C. T., Quénol, H., Le Roux, R., Gendig, E., and Schulmann, T.: The application of high-resolution atmospheric modelling to weather and climate variability in vineyard regions, OENO One, 51, 99-105, 10.20870/oeno-one.2016.0.0.1538, 2017.

Trömel, S., and Schönwiese, C. D.: Probability change of extreme precipitation observed from 1901 to 2000 in Germany, Theoretical and Applied Climatology, 87, 29-39, 10.1007/s00704-005-0230-4, 2007.

van der Linden, P., and Mitchell, J. F. B.: ENSEMBLES: Climate Change and its Impacts: Summary of research and results from the ENSEMBLES project., Met Office Hadley Centre, FitzRoy Road, Exeter EX1 3 PB, UK., 160pp., 160 pp., 2009.

Van Leeuwen, C., and Seguin, G.: Incidences de l´alimentation en eau de la vigne, appreciée per l´etat hydrique du feuillage, sur le developpement de l´appareil végétatif et la maturation du raisin, Journal of Vine and Wine Sciences, 28, 81-110, 1994.

Van Leeuwen, C., and Destrac-Irvine, A.: Modified grape composition under climate change conditions requires adaptations in the vineyard, OENO One, 51, 147, 10.20870/oeno-one.2016.0.0.1647, 2017.

van Vuuren, D. P., Edmonds, J., Kainuma, M., Riahi, K., Thomson, A., Hibbard, K., Hurtt, G. C., Kram, T., Krey, V., Lamarque, J.-F., Masui, T., Meinshausen, M., Nakicenovic, N., Smith, S. J., and Rose, S. K.: The representative concentration pathways: an overview, Climatic Change, 109, 5, 10.1007/s10584-011-0148-z, 2011.

https://doi.org/10.5194/esd-2021-9
Preprint. Discussion started: 31 March 2021

Vorderbrügge, T., Friedrich, K., Sauer, S., Peter, M., and Miller, R.: Ableitung der FK für Acker aus dem Klassenzeichen der Bodenschätzung, Hesssisches Landesamt für Naturschutz, Umwelt und Geologie, Wiesbaden, 2006.

Webb, L. B., Whetton, P. H., and Barlow, E. W. R.: Modelled impact of future climate change on the phenology of winegrapes in Australia, Australian Journal of Grape and Wine Research, 13, 165-175, DOI 10.1111/j.1755-0238.2007.tb00247.x, 2007.

Webb, L. B., Whetton, P. H., and Barlow, E. W. R.: Observed trends in winegrape maturity in Australia, Global Change Biology, 17, 2707-2719, 10.1111/j.1365-2486.2011.02434.x, 2011.

Wilks, D. S.: Adapting stochastic weather generation algorithms for climate change studies, Climatic Change, 22, 67-84, 10.1007/BF00143344, 1992.

Wild, M.: Global dimming and brightening: A review, J. Geophys. Res., 114, 1-31, 10.1029/2008jd011470, 2009.

Williams, L. E., and Matthews, M. A.: Grapevine, in: Irrigation of Agricultural Crops, edited by: Stewart, B. A., and Nielsen, D. R., ASA-CSSA-SSSA, Madison, WI, 1019-1055, 1990.

WMO: WMO Statement on the State of the Global Climate in 2019, World Meteorological Organization (WMO), 2020.

Wohlfahrt, Y., Smith, J. P., Tittmann, S., Honermeier, B., and Stoll, M.: Primary productivity and physiological responses of *Vitis vinifera* L. cvs. under Free Air Carbon dioxide Enrichment (FACE), European Journal of Agronomy, 101, 149-162, 10.1016/j.eja.2018.09.005, 2018.

Woodward, D. E., Hawkins, R. H., Jiang, R., Hjelmfelt, A. T., and Van Mullem, J. A.: Runoff Curve Number Method: Examination of the Initial Abstraction Ratio, in: World Water Environmental Resources Congress 2003, 1-10, 2003.

Xu, Z., Jiang, Y., Jia, B., and Zhou, G.: Elevated-CO_2 Response of Stomata and Its Dependence on Environmental Factors, Frontiers in Plant Science, 7, 657, 10.3389/fpls.2016.00657, 2016.

Zimmer, T.: Untersuchungen zum Wasserhaushalt von Weinbergsböden im Rheingau, Geisenheimer Berichte, 35, Gesellschaft zur Förderung der Forschungsanstalt Geisenheim, Geisenheim, 232 pp., 1999.